DEVELOPMENT OF Al-Si-Fe/SiC PARTICULATE COMPOSITES AS ADVANCED MATERIALS FOR ENGINEERING APPLICATION

BY

AIGBODION, VICTOR SUNDAY
M.Sc/ENG/48328/05-06

DEPARTMENT OF METALLURGICAL ENGINEERING,
AHMADU BELLO UNIVERSITY, ZARIA
NIGERIA

THESIS SUBMITTED TO THE POST-GRADUATE SCHOOL AHMADU BELLO UNIVERSITY, ZARIA, NIGERIA IN PARTIAL FULFILMENT OF THE REQUIRMENTS FOR THE AWARD OF MASTER OF SCIENCE (M.Sc) DEGREE IN METALLURGICAL ENGINEERING

August, 2007

DECLARATION

I Aigbodion, Victor Sunday hereby declare that this thesis has been conducted by me under the guidance and supervision of my supervisors and has not been presented or accepted at any institution for the award of any degree. All sources of information used in this research work are duly acknowledged in the references.

_____

Aigbodion, Victor Sunday

CERTIFICATION

This thesis entitled "**Development of Ai-S-Fe/SiC Particulate Composites as Advanced Materials for Engineering Application"** by Aigbodion. Victor Sunday meets the regulation governing the award of Master of Science in Metallurgical Engineering of Ahmadu Bello University, Zaria and is approved for its contribution to knowledge and literary presentation.

_____ _____

Engr. Dr. S.B. Hassan Date
(Chairman, Supervisory Committee)

_____ _____

Engr. Dr. O. Aponbiede Date
(Member, Supervisory Committee)

_____ _____

Engr. Dr. S.B. Hassan Date
(Head of Department)

_____ _____

Dean, Post-Graduate School Date

ACKNOWLEDGEMENT

This thesis could not have been completed without the guidance and direction from my supervisors; Engr. Dr. S.B. Hassan and Engr. Dr. O. Aponbiede who aided from start to finish with advice on everything from test procedure to data analysis, your kind gesture shall always remain fresh in my mind, for giving my life a purpose.

My appreciation also goes to all the staff of Metals Department, National Metallurgical Development Centre, Jos, for their constant help during the production and preparation of my Metallurgical test, may the almighty God reward every one of you abundantly in Jesus name Amen.

I would like to thank Dr. S. A. Yaro for his direction and assistance in this research work, may the good lord bless you. Also, I am very grateful, for all the criticisms and Technical assistance received from the entire post-graduate Lecturer in the Department of Metallurgical Engineering, A.B.U, Zaria.

1 would like to thank my colleagues and friends for their cooperation and continuous encouragement. Also, I am especially grateful to Chief and Mrs Jerry Okpanachi and my brothers and sisters, for their continuous support and advice. I am very grateful to the love of my heart Miss Vera Ije for the support and care giving to me during the course of this programme. Finally, I give thanks to my parent for their care and encouragement.

May God bless you all Amen.

ABSTRACT

This work has been carried out to develop a particulate strengthened Al-Si-Fe composites using silicon carbide as the particulate. Al-Si-Fe alloy with 5-25 weight percent silicon carbide particles were produced using the double stir casting method. The composites were heat-treated at 500^{o}C for 3hours and quenched in warm water at 65^{o}C, aged at100, 200 and 300^{o}C with various ageing times between 60 to 660minutes. The microstructures of the various alloy particulate composites produced were examined. The physical and mechanical properties measured include: densities, porosity, ageing kinetic, ultimate tensile strength, yield strength, hardness values and impact energy. The result obtained reveals hardness values and activation energy of diffusion increased with increase in the weight fraction of silicon carbide and accelerates the kinetic of ageing. The yield strength and ultimate tensile strength increased by a maximum of 20% silicon carbide addition with general decrease in impact energy. These results show that at 20% silicon carbide addition the composites has 9.15%, 17.79%, 29.17% and 29.85% increases in yield strength, tensile strength, impact energy and hardness respectively over that of the as-cast samples at peak ageing of 200^{O}C. The increases in mechanical properties (tensile, impact and hardness) during ageing, was attributed to formation of a coherent and uniform precipitation of the second phase in the matrix of the metal, which resulting from increase in the dislocation density at the particles-matrix

interfaces. These results show that the Al-Si-Fe alloy has been well enhanced by the addition of silicon carbide using double stir casting method.

TABLE OF CONTENTS

TITLE PAGE----------i

DECLARATION----------ii

CERTIFICATION----------iii

ACKNOWLEDGEMENT----------iv

ABSTRACT----------v

TABLE OF CONTENTS----------vi

LIST OF TABLES----------x

LIST OF MICROGRAPHS(APPENDIX A)----------xii

LIST OF FIGURES(APPENDIX B)----------xiv

LIST OF PLATES (APPENDIX C)----------xv

CHAPTER ONE----------1

1.0 Introduction----------1

CHAPTER TWO----------6

2. 0 Literature Review----------6

2.1Aluminium Matrix composites (AMCS)----------6

2.2 Al-Si-Fe Alloy System----------7

2.3 Properties of Aluminium Matrix composites (AMCS) ----------8

2.4 Types of Aluminium Matrix composites AMCs----------10

2.4.1 Particle Reinforced Aluminium Matrix Composites (PAMCs)----------10

2.4.2 Short Fibre- And Whisker-Reinforced Aluminium Matrix Composites-------12 2.4.3 Continuous Fibre-Reinforced Aluminium Matrix Composites (CFAMCs)----------12

2.4.4 Monofilament Reinforced Aluminium Matrix Composites (MFAMCs)----------13

2.5 Primary processing of AMCs----------13

2.5.1 Liquid state processes----------13

2.5.2 Solid-state processes----------16

2.6 Interfacial Characteristics of AMCs----------18

2.6.1 Physical Phenomena at the Interface----------19

2.6.2 Chemical Reactions at the Interface----------20

2.6.3 Metallurgy of the interfacial area----------23

2.7 Properties of AMCs composites----------25

2.7.1 Physical Properties of AMCs Composite----------25

2.7.2 Mechanical properties of AMCs Composites----------28

2.7.3 Wear Resistance----------33

2.7.4 Corrosion Resistance----------34

2.8 Effect of ceramic reinforcements on the behavior of aluminium matrix in AMCs---35 2.8.1 Intrinsic Effects Ceramic Reinforcements----------35

2.8.2 Extrinsic Effects of Ceramic Reinforcement----------36

2.9 Thermal treatments of AMCs----------36

2.9.1 Age Hardening Characteristics of Ceramic Reinforced Aluminium Alloys---36

2.9.2 Principles of Age Hardening of Aluminium alloys/composites----------40

2.9.3 Kinetic Analysis of Precipitation Reactions----------41

2.10 Applications of AMCs----------44

CHAPTER THREE----------47

3.0 Materials and Methods----------47

3.1 Materials----------47

3.2 Equipment----------47

3.3 Methods----------47

3.3.1 Samples production----------47

3.3.2 Heat treatment of the samples----------49

3.3.3 Determination of Density----------49

3.3.4 Determination Apparent Porosity----------50

3.3.5 Hardness values determination----------50

3.3.6 Determination of the Tensile properties----------51

3.3.7 Impact Strength Determination*----------*51

3.3.8 Microstructural Examination----------52

CHAPTER FOUR----------53

4.0 Results and Discussion ----------53

4.1 Physical Properties of Al-Si-Fe/Sic Composites----------53

4.1.1 Macrostructural analysis----------53

4.1.2 Density----------53

4.1.3 Apparent Porosity----------54

4.2 Kinetic characteristics of ageing----------55

4.2.1 Statistical analysis of the ageing process---------58

4.3 Microstructural analysis----------62

4.4 Mechanical Properties of Al-Si-Fe/SiC Composites----------63

4.4.1 Hardness Values----------63

4.4.2 Yield and Tensile Strengths----------64

4.4.3 Percentage Elongation ----------67

4.4.4 Impact energy----------68

CHAPTER FIVE----------69

5.0 Conclusions and Recommendations----------69

5.1 Conclusions----------69

5.2 Recommendations----------72

REFERENCES ----------73

APPENDIX A (Micrographs)----------78

APPENDIX B(Figures)----------90

APPENDIX C(Plates)----------97

LIST OF TABLES

Table 2.1 Interfacial Reactions----------22

Table 4.1, Result of density with percentage of SiC----------53

Table 4.2, Result of porosity with percentage of SiC----------54

Table 4.3, Result of Kinetics analysis with percentage of SiC----------55

Table 4.4, Result of acceleration to precipitation hardening(R) with percentage of SiC----------56

Table 4.5, Result of hardness (HRB) characteristics at $100^{O}C$ with percentage of SiC----------57

Table 4.6, Result of hardness (HRB) characteristics at $200^{O}C$ with percentage of SiC --57

Table 4.7,Result of hardness (HRB) characteristics at $300^{O}C$ with percentage of SiC----57

Table 4.8 : Statistical design of the ageing process----------58

Table 4.9: Factorial design of the ageing process showing treatment combination-------59

Table 4.10: Experimental conditions and Hardness values for each given condition-----59

Table 4.11: Yates analysis table----------60

Table 4.12:Analysis of variance of the effects----------61

Table 4.13, Result of hardness (HRB) for As cast and aged hardened with percentage of SiC----------63

Table 4.14: Result of the Tensile strength N/mm^2 of Al-Si-Fe/SiC composites with percentage silicon carbide----------64

Table 4.15: Result of the Yield strength N/mm^2 of Al-Si-Fe/SiC composites with percentage silicon carbide----------65

Table4.16: Result of the Percentage Elongation of Al-Si-Fe/SiC composites with percentage silicon carbide----------67

Table 4.17, Result of Impact energy for as cast and aged hardened with percentage of SiC----------68

LIST OF MICROGRAPHS (Appendix A)

Micrograph A1, Microstructure of the unreinforced alloy----------78

Micrograph A2, Microstructure of the reinforced alloy(5 wt% of SiC)----------78

Micrograph A3, Microstructure of the reinforced alloy(10 wt% of SiC)----------79

Micrograph A4, Microstructure of the reinforced alloy (15 wt% of SiC)----------79

Micrograph A5, Microstructure of the reinforced alloy (20 wt% of SiC)----------80

Micrograph A6, Microstructure of the reinforced alloy(25 wt% of SiC)----------80

Micrograph A7, Microstructure of the unreinforced alloy after peak aged 100^{O}C-81

Micrograph A8, Microstructure of the unreinforced alloy after peak aged 200^{O}C-81

Micrograph A9, Microstructure of the unreinforced alloy after peak aged at 300^{O}C-----82

Micrograph A10, Microstructure of the reinforced alloy(5 wt% of SiC) after peak aged at 100^{O}C ----------82

Micrograph A11, Microstructure of the reinforced alloy(5 wt% of SiC) after peak aged at 200^{O}C ----------83

Micrograph A12, Microstructure of the reinforced alloy(5 wt% of SiC) after peak aged at 300^{O}C ----------83
Micrograph A13, Microstructure of the reinforced alloy(10 wt% of SiC) after peak aged at 100^{O}C----------84
Micrograph A14, Microstructure of the reinforced alloy(10 wt% of SiC) after peak aged at 200^{O}C----------84
Micrograph A15, Microstructure of the reinforced alloy(10 wt% of SiC) after peak aged at 300^{O}C ----------85
Micrograph A16, Microstructure of the reinforced alloy(15 wt% of SiC) after peak aged at 100^{O}C----------85
Micrograph A17, Microstructure of the reinforced alloy(15 wt% of SiC) after peak aged at 200^{O}C ----------86
Micrograph A18, Microstructure of the reinforced alloy(15 wt% of SiC) after peak aged at 300^{O}C----------86
Micrograph A19, Microstructure of the reinforced alloy(20 wt% of SiC) after peak aged at 100^{O}C ----------87
Micrograph A20, Microstructure of the reinforced alloy(20 wt% of SiC) after peak aged at 200^{O}C ----------87
Micrograph A21, Microstructure of the reinforced alloy(20 wt% of SiC) after peak aged at 300^{O}C ----------88
Micrograph A22, Microstructure of the reinforced alloy(25 wt% of SiC) after peak aged at 100^{O}C----------88

Micrograph A23, Microstructure of the reinforced alloy(25 wt% of SiC) after peak aged at 200^{O}C ----------89
Micrograph A24, Microstructure of the reinforced alloy(25 wt% of SiC) after peak aged at 300^{O}C (x200)----------89

LIST OF FIGURES (Appendix B)

Figure 2.1 Flow Chart on the various method used in producing AMCs----------14

Figure 2.2 some applications of AMCs----------46

Figure B1 Variation of density with weight percentage of SiC addition----------90

Figure B2, Variation of percentage of porosity with weight percentage of SiC addition-90

Figure B3, Plot of 1/t against 1/ T----------91

Figure B4: Variation of activation energy with weight fraction of SiC addition---91

Figure B5: Variation of acceleration to precipitation hardening with weight fraction of SiC at various ageing temperatures----------92

Figure B6: Variation of hardness values with ageing time of the various grades composites at ageing temperature of $100^{O}C$----------92

Figure B7: Variation of hardness values with ageing time of the various grades composites at ageing temperature of $200^{O}C$----------93

Figure B8: Variation of hardness values with ageing time of the various grades composites at ageing temperature of $300^{O}C$----------93

Figure B9: Variation of peaking ageing time with weight fraction of SiC at various ageing temperatures----------94

Figure B10: Variation of hardness values with weight fraction of SiC addition---94

Figure B11: Variation of yield strength with weight fraction of SiC addition------95

Figure B12: Variation of tensile strength with weight fraction of SiC addition----95

Figure B13: Variation of percentage elongation with weight fraction of SiC addition---96

Figure B14: Variation of impact energy with weight fraction of SiC addition--96

LIST OF PLATES (Appendix C)

Plate C1, Materials used in the production of the composites----------97

Plate C2, After pouring of the molten mixture in the prepared sand mould ----97

Plate C3, the produced samples after shaking from the mould ----------98

Plate C4, Macrostructure of the composites after machined for mechanical test--98

CHAPTER ONE

1.0 INTRODUCTION

In the last two decades most research and development efforts have aimed at reinforcing monolithic metals and alloys with a ceramic phase with the primary purpose of enhancing their properties, spanning the domains of physical, mechanical and fracture behaviour (Clyne, 2000, Surappa and Rohatgi, 1981), and strong interest has been shown in the application of metal matrix composites (MMCs) in the design of many engineering and non-engineering components (Maruyama, 1998, Jokinen and Rauta, 1992).

Potential uses of these materials in industries are numerous and they include such areas as aerospace (satellite struts), defensce (electronic instrument racks), automotive (drive shafts and brake discs), sports goods (golf clubs and mountain bicycle frames), and marine (yacht fittings) (Clyne, 2000 and Ikechukwuka, 1997). When compared with the unreinforced aluminium matrix alloy, MMCs in general have superior mechanical properties, such as: high strength, high stiffness, high Wear resistance, and very good elevated temperature properties. These properties can be tailored to meet specific requirements (Skibo et al, 1998).

The early work on MMCs focused mainly on continuous fiber reinforcement. However, high cost of fibers, complex fabrication techniques, and limited fabricability restricted their use to those applications where the end could justify the means (Lloyd, 1999). This opened the way for the development of low cost discontinuously reinforced MMCs, such as particle-reinforced MMCs (Rohatgi et al, 1988, Zhou and Xu, 1997).

Silicon carbide particles have become one of the popular reinforcing phases for many aluminum alloy-based metal matrix composites. They are hard and brittle ceramic particles with high strength, high modulus of elasticity, and high thermal and electrical resistance. The size of the particles depends on both the manufacturer and the type of alloy. However, the mean particle dimension normally lies in the range 2-20μm (Zhou and Xu, 1997).

Particle-reinforced MMCs are produced via various routes. They have additional advantages over the continuous fiber-reinforced MMCs especially since they are low-priced and have both high heat treatment ability and processing flexibility. Particle-reinforced MMCs are now being produced commercially (Zhou and Xu, 1997, Jayalakshmi et al, 2004).

One of the factors limiting the use of MMCs for engineering components is the lack of property characterization in relation to the unreinforced aluminium alloys. The lack of data extends from processing parameters to final mechanical properties. Understanding the factors that influence the physical and mechanical properties of these materials is very important in the sense that these properties are sensitive to the type of reinforcement, the mode of production and the details of post-production processing (Ikechukwuka, 1997).

1.1 BACKGROUND OF THE STUDY

Research on composites, in general, and strong materials in fibre form, in particular, continued for nearly 20 years, until the early 1960s. By then, glass-reinforced plastics were common place, but not very seriously regarded as engineering materials. In both the United States of America (USA) and United Kingdom (UK), continued interest in

composites remained substantially in the hands of the metallurgists who, seeing the inevitable limitations on the thermal stability of metallic alloys (especially for use in gas turbines), were anxious to develop composites reinforced with metallic reinforcements(Mbaya, 2005).

By the early 1960s, however, interest in MMC waned rapidly, until the early 1980s. At the end of the 1970s, however, a great deal of work was in progress on MMCs in the USA, but a US-government embargo on the transmission of strategic information outside the country prevented general knowledge of the details of this work. Even at international conferences in the USA, it became common to hold closed sessions to which non-nationals could not gain access, at which MMC work was discussed (Donne et al, 1990, Mbaya, 2005)

Currently, however, there is a renewed activity in metal-matrix composites (MMC) development which focuses more on particulates, than the Fibre-reinforced ones. A number of organizations in the western world, particularly, are now developing all kinds of particulate MMCs; a class of materials that was formerly familiar to metallurgists as "cermets" (Mbaya, 2005).

Particle-reinforced MMCs have been produced for research at universities roughly since the 1960's. Powder metallurgical production of these materials in experimental or prototype quantities followed several decades later, resulting in the birth of a powder metallurgical production base for these materials (Donne et al, 1990). A second impetus behind the development of these materials was the proposal by Skibo and Schuster in the 1980's of a process for their production using molten metal instead of far more expensive solid powder metal (Donne et al, 1990). The major problem in this technology is to

obtain sufficient wetting of dispersoid by the liquid metal and to get a homogeneous dispersion of the ceramic particles. Several structural defects such as porosity, particle clusters, oxide inclusions and interfacial reactions were found to arise from the unsatisfactory casting technology (Rohatgi et al, 1988). Among all the liquid-state processes, stir-casting technology is considered to be the most potential method for engineering application in terms of production capacity and cost efficiency. This method is very attractive to the developing country like Nigeria because of the possibility of using the convectional foundry equipment.

1.2 STATEMENT OF PROBLEM

In particular to Al-Si matrix composite, problem of wettability and interfacial reactions has being reported by several researchers during the production of this composite using the liquid method. Also the possibility of using Al-Si-Fe matrix with low silicon and iron content has not been studied, including their ageing characteristics.

1.3 AIMS AND OBJECTIVES OF THE STUDY

The aims and objectives of this present research are as follows:

1) To use double stirring method and covering fluxes with the hope of producing Al-Si-Fe/SiC cast composites with better particle distribution.
2) To examine properties such as density and porosity of the produced composites with the percentage increase in SiC.
3) To investigate the influence of SiC-particle reinforcement on the precipitation hardening behavior of the cast composites using the mechanical properties and microstructure, as criteria.
4) To create awareness, and stimulate interest, on the use of aluminium matrix

Composites for engineering applications. This consideration is particularly important because of the roles composites are now playing in engineering and many other applications, in more recent times.

1.4 **SIGNIFICANCE OF THE STUDY**

The significance of this work is to further exploit the properties, characteristics and potentials of aluminium, in order to compliment its existing areas of application, as well as to determine new areas of application (such as its use in composites) to increase the possible areas and ways of utilizing aluminium metal and it alloys.

1.5 **LIMITATION OF THE STUDY**

Because of the lack of availability of equipment for now, the following analyses could not be done during the course of this research

1) Scanning electron microscopy (HRSEM) or high-resolution transmission electron microscopy (HRTEM) for further determination of the ageing characteristics
2) Determination of the amount of Al_4C_3 form.
3) Differential scanning calorimetry (DSC) and electrical resistivity measurements
4) The fatigue and creep properties could not be determined.

CHAPTER TWO

2. 0 LITERATURE REVIEW

2. 1 ALUMINIUM MATRIX COMPOSITES (AMCs)

The term "composite" broadly refers to a material system which is composed of a discrete constituent (the reinforcement) distributed in a continuous phase (the matrix), and which derives its distinguishing characteristics from the properties of its constituents, from the geometry and architecture of the constituents, and from the properties of the boundaries (interfaces) between different constituents (Clyne, 2000 and Ikechukwuka, 1997). Composite materials are usually classified on the basis of the physical or chemical nature of the matrix phase, e.g., polymer matrix, metal-matrix and ceramic composites. In addition there are some reports to indicate the emergence of intermetallic-matrix and carbon-matrix composite (Surappa and Rohatgi, 1981).

Aluminum is the most popular matrix for the metal matrix composites (MMCs). The aluminium alloys are quite attractive due to their low density, their capability to be strengthened by precipitation, their good corrosion resistance, high thermal and electrical conductivity, and their high damping capacity (Whitehouse et al., 1991). Aluminum matrix composites (AMCs) have been widely studied since the 1920s and are now used in sporting goods, electronic packaging, armours and automotive industries (Skibo et al, 1988 and Donne et al, 1990). They offer a large variety of mechanical properties depending on the chemical composition of the aluminium-matrix. The following reinforcements Al_2O_3, SiC, C, SiO_2, B, BN, B_4C are usually used in aluminium matrices (Ikechukwuka, 1997; Skibo et al, 1988 and Lloyd, 1999). As proposed by the American

Aluminum Association the AMCs should be designated by their constituents: accepted designation of the matrix / abbreviation of the reinforcement's designation / arrangement and volume fraction in % with symbol of type (shape) of reinforcement. For example, an aluminum alloy AA6061 reinforced by particulates of alumina, 22 % volume fraction, is designated as "AA6061/ Al_2O_3 /22p" (Ikechukwuka, 1997; Rohatgi et al, 1988, Zhou and Xu, 1997)

2.2 Al-Si-Fe ALLOY SYSTEM

The presence of Si and Fe in aluminium causes various precipitates to form during solidification of the alloys. During the solidification of the alloys system, development of dendritic network, precipitation of Al_3Fe-containing phase and formation of complex eutectic phases containing $Al_3(FeSi)$ occur (Metals handbook, 1979)

The common occurring phases are the α (Fe-Si) and the β (Fe-Si) represented as $FeSiAl_3$ the former occurring in low silicon alloys as Chinese-script and the latter occurring in the form of plates in high silicon-iron-aluminium alloys (13% silicon) the β constituent is generally thin and curved when the iron content is comparatively low, but with higher iron content they tend to become straight (Rajan and Sharma, 1988).

In the sand and permanent mould aluminium silicon alloy casting, iron is limited to 0.9% maximum if the iron content exceeds this limit large plates of β (Fe-Si) are formed which causes the castings to be extremely brittle (Metals handbook, 1979).

The composition specification of these alloys rests mainly on the iron and silicon. Iron increases strength and hardness, reduces tendency toward hot cracking. Silicon improves the fluidity of the molten metal as well as to improve casting quality and mechanical properties (Metals handbook, 1979).

2.3 PROPERTIES OF ALUMINIUM MATRIX COMPOSITES (AMCs)

The major advantages of AMCs compared to unreinforced aluminium alloy are as follows (Clyne, 2000; Surappa and Rohatgi, 198, Whitehouse et al, 1991):

I. Greater strength
II. Improved stiffness
III. Reduced density (weight)
IV. Improved high temperature properties
V. Controlled thermal expansion coefficient
VI. Thermal/heat management
VII. Enhanced and tailored electrical performance
VIII. Improved abrasion and wear resistance
IX. Control of mass (especially in reciprocating applications)
X. Improved damping capabilities.

These advantages are quantified for better appreciation. For example, elastic modulus of pure aluminium can be enhanced from 70GPa to 240GPa by reinforcing with 60 vol.% continuous aluminum fibers. On the other hand incorporation of 60 vol% alumina fibre in pure aluminium leads to decrease in the coefficient of expansion (Jayalakshmi et al, 2004). Similarly it is possible to process Al-9%Si-20vol% SiC particulates composites

having wear resistance equivalent or better than that of grey cast iron (Clyne, 2000). All these examples illustrate that it is possible to alter several technological properties of aluminium/aluminium alloy by more than two–three orders of magnitude by incorporating appropriate reinforcement in suitable volume fraction (Rohatgi et al, 1988 and Asthana, 1998). AMCs material systems offer superior combination of properties in such a manner that today no existing monolithic material can rival (Whitehouse et al., 1991). Over the years, AMCs have been tried and used in numerous structural, non-structural and functional applications in different engineering sectors (Jokinen and Rauta, 1992; Ikecukwuka, 1997 and Lloyd, 1999). Driving force for the utilization of AMCs in these sectors include performance, economic and environmental benefits. The key benefits of AMCs in transportation sector are lower fuel consumption, less noise and lower airborne emissions (Lloyd, 1999). With increasing stringent environmental regulations and emphasis on improved fuel economy, use of AMCs in transport sector will be inevitable (Surappa and Rohatgi, 1981).

AMCs are intended to substitute monolithic materials including aluminium alloys, ferrous alloys, titanium alloys and polymer based composites in several applications. In order that AMCs substitution for monolithic materials in engineering system is wide spread, there is a compelling need to redesign the whole system to gain additional weight and volume savings (Lloyd, 1999 and Rohatgi et al, 1988). In fact according to the UK Advisory Council on Science and Technology, AMCs can be viewed either as a replacement for existing materials, but with superior properties, or as a means of enabling radical changes in system or product design. Moreover, by utilizing near-net shape forming and selective-reinforcement techniques, AMCs can offer economically

viable solutions for wide variety of commercial applications (Maruyama, 1998). Recent successes in commercial and military applications of AMCs are based partly on such innovative changes made in the component design. Lack of knowledge and information about utilization possibilities, service properties has hindered the wider usage of AMCs.

2.4 TYPES OF AMCs

AMCs can be classified into four types depending, on the type of reinforcement (Clyne, 2000 and Ikechukwuka, 1997).

a) Particle reinforced aluminium matrix composites (PAMCs)
b) Short fibre- and whisker-reinforced aluminium matrix composites (SFAMCs)
c) Continuous fibre-reinforced aluminium matrix composites (CFAMCs)
d) Monofilament reinforced aluminium matrix composites (MFAMCs)

2.4.1 Particle Reinforced Aluminium Matrix Composites (PAMCs)

Particulate Reinforced Aluminium Metals" or "Particle Reinforced Metals" (PAMC's) are combinations of a metal or alloy with a finite volume fraction of a roughly equiaxed second phase, generally ceramic, that is deliberately introduced into the metal in order to improve its properties. Frequent motivations are to raise the modulus, improve wear resistance, or lower the thermal expansion of aluminium while preserving its low density (silicon carbide particle reinforced aluminium serves as an example) (Clyne, 2000 and Maruyama, 1998).

Generally, the improvements that are achieved in the properties of the metal are less extensive than with fibrous reinforcements; however, besides the lower cost, these

materials present the additional advantages of having generally isotropic properties, and of being overall compatible with most metalworking processes (machining, deformation processing, welding), particularly when the volume fraction ceramic is below about 30 pct (Jokinen and Rauta, 1992, Clyne, 2000).

Particulate reinforcements added to metals are generally ceramic in nature, although in some cases a refractory metal is used (tungsten in copper is an example). The reinforcing particles must, in order to be viable for a given metal, fulfill the following requirements.

(i) They must be comparatively inexpensive. This requirement generally defines both the nature and the form of the particulate reinforcements used in producing engineering PAMCs

(ii) The matrix and the reinforcement must not be too mutually reactive (unless an in-situ composite is to be produced): given the intimacy of contact between matrix and reinforcement in the composite, the ceramic must thus be chemically stable in contact with the metal.

Generally, no interfacial reaction is desired, as matrix/particle bonding is in many systems inherently strong without reaction (i.e., involves chemical bonds crossing the interface) and is weakened by a finite layer of brittle reaction product(s); hence, systems used are essentially ones of low or nil chemical reactivity.

(iii) The reinforcement must of course also improve the matrix properties.

These preconditions generally narrow the list of candidate reinforcements to only a few possibilities. For the reinforcement of aluminium and its alloys, silica or reinforcements

with a significant fraction of silicon (mullite, for example) are not optimal because of (i) their reactivity with the matrix (aluminium and magnesium both reduce silica) and (ii) their relatively low elastic modulus compared with that of several alternative ceramics. The two main ceramic particles used as reinforcements for aluminium are: silicon carbide, alumina e.t.c (Clyne, 2000 and Skibo et al, 1988)

2.4.2 Short Fibre- And Whisker-Reinforced Aluminium Matrix Composites (SFAMCs*)*

These contain reinforcements with an aspect ratio of greater than 5, but are not continuous. Short alumina fibre reinforced aluminium matrix composites is one of the first and most popular AMCs to be developed and used in pistons. Whisker reinforced composites are produced either by Powder Metallurgy processing or by infiltration route.

Mechanical properties of whisker-reinforced composites are superior compared to particle or short fibre reinforced composites. However, in the recent years, usage of whiskers as reinforcements in AMCs is fading due to perceived health hazards and hence of late, commercial exploitation of whisker-reinforced composites has been very limited. Short fibre reinforced AMCs display characteristics in between that of continuous fibre and particle reinforced AMCs (Clyne, 2000).

2.4.3 Continuous Fibre-Reinforced Aluminium Matrix Composites (CFAMCs)

In continuous fibre reinforcements, the reinforcements are in the form of continuous fibres (of alumina, Silicon carbide or carbon). The fibres can either be parallel or pre-woven, braided prior to the production of the composite. AMCs having fibre volume fraction up to 40% are produced by squeeze infiltration technique (Clyne, 2000).

2.4.4 Monofilament Reinforced Aluminium Matrix Composites (MFAMCs)

Monofilaments are large diameter (100 to 150 μm) fibres, usually produced by chemical vapour deposition (CVD) of either silicon carbide or boron into a core of carbon fibre. Bending flexibility of monofilaments is low compared to multifilament. monofilament reinforced aluminium matrix composites are produced by diffusion bonding techniques, and is limited to super plastic forming aluminium alloy matrices. In continuous fibre-reinforced aluminium matrix composites and monofilament reinforced aluminium matrix composites the reinforcement is the principal load-bearing constituent, and the role of aluminium matrix is to bond the reinforcement transfer and distribute load. These composites exhibit directionality and have low strength in the direction perpendicular to the fibre orientation (Ikechukwuka, 1997).

2.5 PRIMARY PROCESSING OF AMCs

Figure 2.1 shows the primary processes of manufacturing of aluminium metal composites at industrial scale which can be classified into two main groups: Solid and liquid state processes (Clyne, 2000; Surappa and Rohatgi, 1981 and Ikechukwuka, 1997).

2.5.1 Liquid state processes.

In the liquid matrix method, three main processes can be used to combine metal and particles. In the first, the particles are stirred into the molten matrix e.g. Duralcan composites production. Besides avoiding matrix/reinforcement chemical interaction, the principal difficulty with this process is that the molten metallic matrix does generally not wet the ceramic particles. For this reason, mechanical force is often used to stir the particles into the matrix: this is done in the Duralcan process using specialized equipment (Clyne, 2000). Since the resulting composite slurry, must at all times flow in order for

stirring to be possible, the volume fraction reinforcement that is added in this process is generally below around 30-40%. Above this value, the slurry becomes a thick paste, which does not flow and hence, it is hard to process or cast (Clyne, 2000).

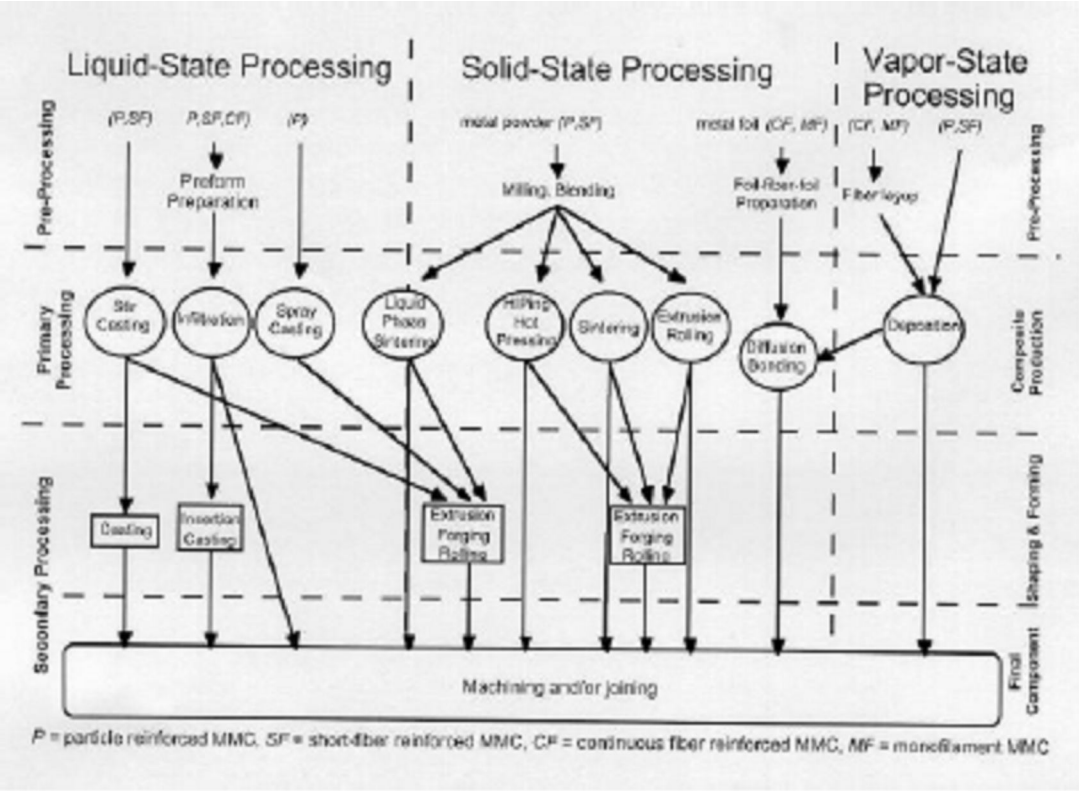


Figure 2.1: Metal Matrix Composites (MMCs) Manufacturing Techniques

Source: Clyne, 2000.

Stir-cast composites are in practice generally reinforced with up to about 25% ceramic particles, to keep the ductility above a certain level (of one to a few percent).

Variants of the process exist, one of which is called "compocasting", which uses a semi-solid instead of fully molten matrix, and another is referred to as “vortex method", used in research by some groups, which consists in vigorously stirring the matrix and adding the particles in the vortex. Resulting composite slurries are subsequently cast into

ingots or billets, for subsequent remelting and casting or for deformation processing, respectively (Surappa and Rohatgi, 1981, Clyne, 2000).

The second main liquid metal process used for the production of particle reinforced metals is infiltration: In this process, a preform of the reinforcement is produced, held together either by a binder or within a mold, and the molten metal matrix is caused to flow into the open pore space left between the particles in the preform. Again, matrices generally do not wet the particles, although exceptions exist, particularly in metal/metal systems, e.g. (i) tungsten particle preforms infiltrated with copper, and (ii) porous steel powder compacts, also infiltrated with copper. As a consequence, the matrix must either be forced into the preform, or alternatively chemical means must be used to improve wetting to the point where the matrix spontaneously invades the pores within the perform (Ikechukwuka, 1997).

one example of this latter strategy is the Lanxide Primex™ process, which uses a nitrogen-containing atmosphere and magnesium additions to the molten matrix to promote spontaneous infiltration of preforms of various ceramic reinforcements, such as SiC particle (Surappa and Rohatgi, 1981).

When chemical means are not employed, pressure is applied onto the metal using several means. With particle reinforced metals the main processes used are squeeze casting (used to produce automotive engine components, for example "Lokasil™" Si particle reinforced cylinder liners in aluminium engine blocks), and pressure infiltration. This latter process uses pressurized gas within a high-temperature pressure chamber; it is used in the production of net-shape components. Generally, electronic substrates for the electronics industry are produced in this way (Clyne, 2000).

Because the reinforcement particles must form, before infiltration, a self-sustaining porous solid preform, volume fractions ceramic particle are generally high in infiltrated AMCs, these are nearly always above 40%, and can be raised using multimodal particle blends to values in the neighbourhood of 70%. Al-Si alloys reinforced with about 70% SiC are particularly interesting for the production of electronic substrates because of the low coefficient of thermal expansion that can be achieved with such high ceramic contents. Infiltration is thus the principal production method for composites used in electronic packaging. Given the high fraction ceramic, infiltrated AMCs cannot be deformed and are seldom machined. Net shape processing is therefore important and largely dictates the selection of the process employed (e.g., gas-pressure infiltration) Lower volume fractions ceramic have, however, been produced via infiltration by some producers using different means either by diluting infiltrated composites into more metal, or directly, using sub-micron particles packed in preforms containing less than 40% vol. reinforcement (Clyne, 2000 and Ikechukwuka, 1997).

2.5.2 Solid-state processes

Solid-state densification is the second principal method of producing AMCs. Essentially, it involves the use of conventional powder metallurgical processing, with the initial powder blend containing a fraction of ceramic particles blended with the metal powder. Provided the ceramic is chemically inert in contact with the metal during densification, densification and subsequent shaping processes similar to those used in powder metallurgical processing of the unreinforced matrix alloy can be used.

The presence of the reinforcement has influence on the rate and ease of densification of the matrix metal powder. The reinforcement being stiffer than the matrix will

generally carry a significant fraction of applied stress onto the powder compact. The reinforcement therefore inherently slows all pressure-densification processes. Also, since the ceramic particles generally retain their initial shape in the powder blend, sintering at metal/ceramic particle contacts is slower than at metal/metal contacts, hence, the presence of ceramic particle also slows down high-temperature sintering processes as well (Clyne, 2000 and Ikechukwuka, 1997).

Furthermore, if the reinforcement is initially present at a volume fraction sufficiently high to generate a three-dimensionally self-sustaining network of ceramic/ceramic particle contacts, densification of the powder compact may be hindered significantly, or prevented altogether. There is, therefore, an upper limit on the volume fraction of ceramic powder particles that can reinforce metals in AMCs produced by powder metallurgy. An important variable in this regard is the ratio of ceramic to metal powder particle radii. The higher this ratio, the higher the volume fraction ceramic that can be incorporated into the composite before ceramic/ceramic particle bridges form a self-sustaining network (Clyne, 2000 and Jayalakshmi et al, 2004).

In practice, volume fractions ceramic up to about 55% have been produced by powder metallurgical means; however, ceramic contents rarely exceed 35% in practice. The ceramic particles diameter can vary from millimetric down to nanometric dimensions. Densification can be achieved using a variety of processes, involving diverse cycles of stress and temperature applied on compacts of the powders sealed within an evacuated can. For aluminium and magnesium-based matrix composites, as in densification of unreinforced matrix powder, intense shear of the powder compact or

specific modification of the aluminium powder is required in order to break up the oxide scale that covers the metal particles and prevents metal powder densification.

Processes therefore often include steps involving high deformation, such as extrusion or rolling, when producing particle reinforced aluminium or magnesium alloys. With other matrix systems, including alloys based on titanium and steel, isostatic processes, such as Cold Isostatic Pressing (CIP) followed by sintering or Hot Isostatic Pressing (HIP), are used. After densification, conventional deformation processes such as extrusion and forging are employed to give its final shape to the composite (Clyne, 2000 and Ikechukwuka, 1997).

2.6 INTERFACIAL CHARACTERISTICS OF AMCs

Metal matrix composites (MMCs) consist of an intricate structure of metals and an inorganic reinforcing material. The frontier zone between these two phases (interface or interphase) is one essential part of MMCs. Bonding develops from physical or chemical interactions, interfacial frictional stress and thermal stresses due to mismatch between coefficient of thermal expansion of reinforcement and matrix (Lloyd et al., 1990; Ribes et al, 1990 and Lepetitcorps et al, 1991). The understanding and control of the underlying interfacial phenomena governing the transmission of thermal, electrical, and mechanical properties across the whole composite might become of paramount importance when designing AMCs for a particular task. Among the various routes available for the processing of AMCs, two main categories can be distinguished, namely liquid phase processing involving molten metals such as melt stirring or melt infiltration and solid state processing via powder metallurgy. The interfacial problem is much more

of a concern in the liquid phase processing due to inherent process peculiarities (Ribes et al., 1990 and Lepetitcorps et al, 1991).

In the case of continuous fibre reinforced metals (CFRM), high strength is achieved by preventing chemical reactions between the matrix and the inorganic fibres. While a weak interface is desirable to enhance longitudinal strength and toughness, a strong interface is desirable to achieve good transverse properties in CFRM. A weak interface will lead to crack propagation following the interface, while a strong matrix associated with a strong interface will reveal cracks across both the matrix and the reinforcements. If however the matrix is weak in comparison with both the interface and the particle strength, the failure will propagate through the matrix itself (Lloyd et al, 1990).

2.6.1 Physical Phenomena at the Interface

The wettability of the reinforcement material by the liquid metallic matrix plays a major role in the bonding formation. It mainly depends on heat of formation, electronic structure of the reinforcement and the molten metal, temperature, time, atmosphere, roughness and crystallography of the reinforcement. Similarity between metallic and covalent bonding is reflected in that some metal-like solids (TiC, ZrC) are more easily wetted than strongly ionic ceramics such as alumina that remains poorly wetted (King, 1987, Zhou and Xu, 1997).

Surface roughness of the reinforcing material improves the mechanical interlocking at the interface, though the contribution of the resulting interfacial shear strength is secondary compared to chemical bonding. Large differences in thermal expansion coefficient between the matrix and the reinforcement should be avoided as

they can induce internal matrix stresses and ultimately give rise to interfacial failures (Lloyd et al, 1990).

2.6.2 Chemical Reactions at the Interface

Selected examples of interfacial reactions encountered in MMCs are given in Table 2.1. Form a purely thermodynamical point of view, a comparison of free enthalpy of formation at various temperatures shows that many metals in the liquid state are reactive toward the reinforcing materials in particular oxides or carbides. In some cases, such as for Al-SiC, the reactivity even persists below the solidus line failures (Ribes et al, 1990 and Lloyd et al, 1990).

The chemical processes involved here are the oxidation of one element from the matrix and the reduction of the reinforcing materials. Though thermodynamically favoured, some reactions are however not observed and practically the kinetics of these reactions has to be considered in conjunction with thermodynamic data in order to evaluate the real potential of the reactions (Nardone and Prewo, 1986). The consequences of such interfacial reactions are the chemical degradation of the reinforcing material associated with a decrease of its mechanical properties, the formation of brittle reaction products at the interface, as well as the release of elements initially part of the reinforcing material toward the matrix may generate important metallurgical phases at the vicinity of the reinforcing materials (King, 1987). Moreover in the case of alloyed matrices, the selective reactivity and depletion of given elements from the alloy can generate compositional gradients in the matrix and may therefore alter its properties close to the interface.

In the case of AlMgSi(AA6061)-alumina the depletion of Mg in the interphase region due to the formation of spinel alters subsequent solution-hardening treatments. For AlMg-SiC, the release of Si during the interfacial reaction engenders the formation of new intermetallics such as Mg_2Si. Though a moderate reaction may improve the composite bonding, extended reactions usually ruin the reinforcing material. The relation between interfacial reactions and interface strength depends on the materials, for example, Mg-C presents a weak interface, whereas the Al- alumina Altex™ couple possesses a strong interfacial bonding despite the absence of chemical reaction (Leptitcorps et al, 1991).

Table 2.1 Interfacial Reactions.

Reactivity of selected reinforcement materials with Al and Mg [Al] Likely to be observed < 8000c in MMC processing							
			Al	Mg +Al	Mg	Cu	Ti
C			4AI +3C= AI C $_3$	2 AI + Mg+2 C=AI_2 MgC_2 [<2 % AI) 4 AI+ 3C =AI_4 C_3 {>2% AI)	no reaction	no reaction	Ti +C=TiC
Si			AI Si alloy formed	Si +2M=Mg2 Si	Si+2Mg---Mg_2Si	no data	no data
	B_4C		6B_4 C+ 27 AI= 6A I_3 B C+ 9AIB_2 AI B_{10} AI_3 $B_{48}C_2$ $AIB_{24}C_4$ also formed	6B_4C+27AI=6AI_3BC+9AB_2 AIB_{10}, $AIB_{24}C_4$ also formed	no data	no data	no data
	SiC		4AI+3SiC=AI_4 C_3 +3Si	4AI+3SiC=AI_4C_3+3Si	No data	no reaction	SiC+Ti-=TiC+Si
	TiC		4 AI+3TiC= AI_4C_3+3Ti 13AI+3TiC=AI_4C_3+3AI_3Ti	No data	no data	no data	no data
		AI_2O_3	no reaction	3Mg+4AI_2O_3=3$MgAI_2O_4$+2AI 3Mg+AI_2O_3-3MgO+2AI	3Mg+4AI_2O_3=3$MgAI_2O_4$+2AI	no data	no data
		SiO_2	no reaction	Mg+2SiO_2+2AI=$MgAI_2O_4$+ 2Si 2$MgAl_2O_4$+3Si=2MgO+3SiO_2 +4AI	2Mg+SiO_2=2MgO+2Si	no data	no data

Sources: Ribes et al, 1990 and Lloyd et al, 1990.

2.6.3 Metallurgy of the interfacial area

The elaboration of MMCs requires often a very short solidification time to avoid excess interfacial reaction. During the cooling process, differences in thermal capacity and conductivity between the reinforcing material and the matrix induce localized temperature gradients. Solidification of the metallic matrix is believed to be generally a directional outward process, starting from the inside of the metallic matrix while ending at the reinforcing material surface. Heterogeneities such as insoluble precipitates or enriched phases are often found concentrated at the interface and grain boundaries when working with alloys (Cu-, Si-containing Al alloys). Depending on the alloy, undesired phases could be dissolved by a subsequent heat treatment. Commercial alloys containing Ti, Zr, Mn as "grain refiner" are usually not suitable matrices for the preparation of MMCs (Lloyd et al, 1990 and Asthana, 1998).

There exist several ways in which the interfacial reactivity can be tuned in metal matrix composites: By acting on the matrix composition, its reactivity toward the reinforcing material can be altered. For example the high reactivity of aluminium toward SiC can be minimized by saturating the aluminium matrix with Si, preventing most of the deleterious Al_4C_3 formation. A surface treatment can be used to passivate the surface of the reinforcing material as exemplified by the system Al-SiC. Here a prior high temperature surface oxidation of SiC to SiO_2 prevents aluminium carbide formation and increases the bonding (Zhou and Xu, , 1997; Ribes et al, 1990, Lepetitcorps et al, 1991).

In the case of Al-Mg-X the interfacial reaction leads to the formation of magnesium oxide and mixed oxides $MgAl_2O_4$ (spinel). In the system AlMg-Al_2O_3 the

formation of spinel is governed by the magnesium content and takes place at 4 <Mg< 8wt%. At higher contents MgO is exclusively formed while spinel formation decreases as Mg is reduced below 4wt% to be virtually non-existance under 1wt% Mg content. However at 1wt% Mg the wetting of particulate alumina is not extensive. Despite its positive effect on interfacial reactions a high content of Mg is however not desirable from the matrix properties point of view. A strategy to avoid brittle spinel formation while maximizing matrix properties is to mix the alumina first with an aluminium matrix having a content of Mg beyond 8wt%, so that a thin passivation layer of MgO is formed at the surface of the alumina. The Mg-content can be decreased at will by adding more aluminium to the melt, while the MgO layer prevents any spinel formation (Lloyd et al, 1990 and Lepetitcorps et al, 1991).

Besides the triggering of interfacial reactions itself, there exist also ways to enhance the poor wettability of reinforcing materials by liquid metals. For example the introduction of a reactive gas in the mixing chamber can lead to wetting improvement. Alternatively raising the temperature at which the mixing is achieved enhances the wetting. In addition, the surface tension of the molten metal can be reduced by traces of alloying elements. Such effects have been reported for aluminium using Pb, Sn, Mg, and Sr, Na. K etc (Lloyd et al, 1990 and King, 1987).

The processing type and parameters have to be selected and adjusted to a particular MMCs system. Metals are generally more reactive in the liquid rather than in the solid state, consequently short processing times, *i.e.* short contact times between the liquid metal and the reinforcement can limit the extend of interfacial reactions (Zhou et al, 1997).

2.7 PROPERTIES OF AMCs COMPOSITES

The enhancement of specific stiffness, specific strength, wear and creep resistance, and the reduction of density and thermal expansivity are a few of the most attractive features of AMCs. Stiffness is a critical design parameter for many engineering components because the avoidance of excessive elastic deflection in service is the principal overriding consideration. A typical potential application of improved creep resistance is in the development of high-temperature components, such as turbine engine parts where the aim is to replace some heavy components with components made of much lighter substitute materials (Nardone and Prewo, 1986; McDanels, 1985, Shi and Arsanault, 1994).

2.7.1 Physical Properties of AMCs Composite

By the combination of a matrix material with reinforcement such as fibers or particles, special physical properties of the material can be achieved. This allows tailoring physical properties of the AMCs material by varying for example the volume content of the inclusion or reinforcement. Therefore the measurement and characterization of physical properties such as density, porosity, Coefficient of Thermal Expansion (CTE), Specific Heat and Thermal conductivity or resistivity plays an important role (Xu and Watt, 1996; Piggott, 1980, Lloyd, 1999).

Additionally requirements to this material class are given through their use under varying temperature conditions. So investigations and observations of physical properties are not only performed at room temperature but also at higher temperatures or under cycling conditions. This is necessary in order to get knowledge of the performance of the material during its use (Xu and Watt, 1996, Piggott, 1980).

2.7.1**.1 Density**

Density of AMCs material can be determined by simply using the relationship between volume and mass. A special technique for the determination of the density where pores are taken into account is the determination by using water displacement (Archimedean density) (Clyne, 2000).

The basic method to determine the dry bulk density is using a specimen with regular shape (usually rectangular). By measuring the mass and with the knowledge of the volume, the density can be calculated using the following expression (Clyne, 2000)

$$\text{Density} = \frac{mass}{volume} \quad (1)$$

The density by the water displacement (Archimedean density) allows the determination of the density in air compared to its displacement in water or other liquid of known density. Depending upon the nature of the specimen (e.g., open or closed pore), the resultant value may deviate from the true mass.

A clean specimen is weighed accurately in air using a laboratory balance. The specimen is then weighed while suspended in water or other liquid of such density that the specimen will sink. Deducting the mass of the suspension wire from the weight in liquid, the volume of the specimen is calculated from the effect of displacement by a liquid of known density (Archimedean principle). This allows the determination of density of specimens with irregular shapes, uneven surfaces, or porosity (Surappa and Rohatgi, 1981, Maruyama, 1998).

2.7.1.**2 Coefficient of Thermal Expansion (CTE)**

Coefficient of Thermal Expansion is one of the most important properties of AMCs. Since nearly all Metal Matrix Composites are used in various temperature ranges, measurement of CTE as a function of temperature is necessary in order to know the behavior of the material. Several different systems for measurement of CTE can be used depending on the temperature conditions. One of the most common used systems is a dilatometer. A dilatometer measures the changes in length of the sample, when the sample in a push rod , an inductive displacement transducer detects dilatometer change in length of the sample. Using various standards and comparison with materials of known expansion, the calibration and corrections of measurements are done. The measurement of the coefficient of thermal expansion (CTE) can be carried out in the temperature range from approx 150°C up to 1500°C under various conditions (air, inert gas or vacuum). CTE can be measured within an error of 3-5% (Jokinen and Rauta, 1992, Clyne, 2000).

2.7.1.3 Porosity

The porosity of AMCs is determined by keeping the composite in the oven at $110^{O}C$ for 3 hours to obtained constant weight W_1. The composite is then suspended in distilled water and boil on a hot plate for 30 minutes, after boiling, while still in hot water, the water is now displaced with cold water and the weight W_2 is measured on a spring balance hinged on a tripod stand. The test sample is then removed from the water and extra water wiped off from the surface by lightly blotting the sample with wet towel and the weight W_3 in air is measured. The porosity of the composites is determined from the relationship below (Clyne, 2000).

$$Pa = \frac{W_3 - W_1}{W_3 - W_2} x100 \quad (2)$$

Pa= porosity

2.7.2 Mechanical Properties of AMCs Composites

Mechanical properties of AMCs, especially the ductility, fracture toughness and fatigue strength, are strongly influenced by the microstructure of the material, such as size, shape and spatial distribution of the reinforcement which is generated during the fabrication and processing (Clyne, 2000). Reinforcing aluminium alloys with ceramic particles produces high strength aluminium matrix composites. This property enables the applicability of AMCs in the aerospace and defense industries, as well as in automotive disk brake rotors, pistons, upper control arms, etc. The strength of a particulate composite is also directly proportional to the hardness of the dispersed particles (particularly at elevated temperatures). This is because, the particles resist the stresses caused by dislocation pile-ups against them (Rohatgi et al, 1988, Nardone and Prewo, 1986).

Particulate in metal matrices can greatly expand the temperature range of use, as well as strengthen the matrix; in the particulates strengthen composites the matrix and particles share the load bearing function (Piggott, 1980). According to Nardone and Prewo (1986) the strengthening effect results from the hydrostatic restraint exerted by the particles, on the movement of the matrix close to it. The author further stated that since the zone of influence of restraint around each particle interacts with another particle over a very limited area only, it is very important that the particles be of small sizes and uniformly distributed, so that the inter-particle spacing become sufficiently small to produce effective strengthening. A second significant driver is the ability to tailor the

mechanical properties through selection of the reinforcement type and volume fraction along with the matrix alloy (Shi and Arsenault, 1994).

2.7.2.1 Stiffness

Elastic modulus is one mechanical property that is always significantly increased by the addition of ceramic particles into a metallic alloy. The enhancement of stiffness achieved by the addition of the reinforcement is retained at high temperatures and this is of great benefit in the design of rotating parts, support members, and structural bodywork. Examples of applications that depend primarily on stiffness include drive shafts, electronic instrument racks, bicycle frames, and inertial guidance spheres for missiles (Vergaard, 1990; Song et al, 1996; Padkin et al, 1987 and Watt et al, 1996).

It should be noted that the rule of mixture (ROM) is appropriate for estimating the Young's modulus of continuous reinforcement, but it overestimates that of discontinuous reinforcement. Therefore, that is why this has been modified in the Halpin-Tsai equation (Nardone and Prewo, 1986, Xu and Arsenault, 1996),

$$E_c = E_m \left(\frac{1 + 2SqV}{1 - qVp} \right) \tag{3}$$

$$q = \frac{\left(\frac{E_p}{E_m} \right)}{\left(\frac{E_p}{E_m + 2S} \right)} \tag{4}$$

Ec, E_m, Ep are the elastic moduli of the composite, matrix, and particle respectively, S is the particle aspect ratio, and *V,* the volume fraction of the particle.

2.7.2.2 Elongation

The major limitation in the engineering properties of particle-reinforced AMCs is the rather low ductility (as quantified by percent elongation). The tensile elongation decreases with increasing particle content as well as with increased aging time in heat treatable alloys (Christman et al, 1989).

The geometry of the reinforcement in MMCs has been shown to rnarkedly affect matrix deformation behavior (Whitehouse et al, 1991; Lloyd, 1991 and Song et al, 1996). This is largely due to the fact that the matrix stress and strain fields developed in response to external loads Vary appreciably with the geometry of the reinforcing phase (Vergaard, 1990*)*. This has, in turn, been shown to alter fracture behavior particularly near the matrix/reinforcement interface. Song *et* al (1996) recently studied the effects of particle shape on the fracture and ductility of a spherical and an angular particle-reinforced 6061 aluminium composite using scanning electron microscopy (SEM) and transmission electron microscopy (TEM). It was found that although the spherical particulate composite showed a slightly lower yield strength and work hardening rate, the ductility was significantly higher than the angular counterpart. The SEM fractographic examination showed that during tensile loading, the spherical composite failed via void nucleation and linking in the matrix near the reinforcement- matrix interface whereas the angular composite failed through particle fracture and matrix ligament rupture. Experimental evidence in the literature shows that voids nucleate preferentially at the sharp corners of the reinforcements (Bayourni et al, 1988).

Recent modeling has predicted that composites with spherical reinforcements have a higher ductility due to the lower matrix triaxiality (Song et al, 1996). Therefore, a

feasible way to improve composite ductility is to use spherical reinforcements to reduce stress concentrations and thereby bring about changes in the stress distribution throughout the composite. The stress distributions created around and within hard particles in a deforming matrix have been studied (Xu and Arsenault, 1996, Watt et al, 1996). The way a particle gather stress to itself depends on the elastic misfit between the two phases. The stress concentrations at sharp corners of the reinforcements give rise to intense localized plastic flow (Christman et al, 1986). The onset of local plastic deformation leads at first to plastic relaxation, but with further deformation, localized strain hardening once again leads to high stresses next to the particles (Watt et al, 1996). Due to the complexity of the stress fields, dislocation glide, void nucleation, and growth in the matrix during plastic deformation proceed differently from those commonly found in unreinforced alloys (Xu and Arsenault, 1996). The particles are known to carry much higher stresses than the matrix. This transfer of stress to the particles and the associated near-particle perturbations affect the failure modes, stiffening, and strength observed in MMCs.

The percentage elongation is determined by fitting together the broken halves of the sample and measuring the distance between the original gauge marks and then it was estimated from the as:

$$\%\text{Elongation} = \frac{L_f - L_0}{L_0} \times 100 \qquad (5)$$

Where
L_f= Final gauge length
L_o= Original gauge length

The percentage reduction in cross-sectional area is determined by measured values of the areas of the necked – down portion of the failed sample and that of the initial/original specimen. The percentage reduction in cross sectional area was then estimated as:

$$\% \text{ RCSA} = \frac{A_0 - A_f}{A_0} \text{ x } 100 \quad (6)$$

Where
Ao = Original cross-sectional area

Af= Final cross-sectional area

2.7.2.3 Tensile Strength

The yield stress is defined as the stress at a plastic strain of 0.2% and represents the limit of the elastic behavior of the composite. Flow stresses are stresses at greater plastic strains. In general the yield stress increases with the fiber/particle volume fraction and a better orientation of the fibers along the tensile axis. The yield stress in compression is in general larger than in tensile due to the residual stress caused by the CTE mismatch between the alloy and the fibers/particle (Vogelsang et al, 1986). The prediction of yielding and flow behavior is quite complex. During tensile loading, at a given strain, the stresses in the matrix are expected to be lower than in the unreinforced alloy due to the load transfer to the reinforcements, and therefore the matrix yielding is delayed in comparison with the unreinforced alloy (work hardening caused by the composite structure) (Xu and Arsenault, 1996).

The yield strength, ultimate tensile strength, percentage elongation and reduction in cross sectional area of alloy/composites are usually determined with the aids of the following relationships (Xu and Arsenault, 1996).

The ultimate tensile strength (UTS) is determined from the formula.

$$\text{UTS} = \frac{P_{\max}}{A_o} \tag{7}$$

Where
Pmax is the maximum load
(A_o) is the original cross sectional area

The convention denoting 0.2% offset is used in determining the yield strength. By drawing a line parallel to the elastic or linear portion of the load-extension curve. The intersection of this line with the load-extension curve gave the yield load (Py) and the ratio of the yield load to the original cross sectional area (A_o) gave the yield strength.

$$\delta_y = \frac{P_Y}{A_o} \tag{8}$$

2. 7.3 Wear Resistance

Although different wear applications require different reinforcement types to achieve optimal wear rate reduction, there are many situations where wear rates are reduced by factors of up to ten by the introduction of the reinforcement. This makes MMCs very attractive for bearings, bushings, cylinder liners, and break rotors. In some cases, it is advantageous to control the distribution of reinforcement so as to provide material of high wear resistance in selected surface areas while other regions are suitably tough, strong, or thermally conducting. This can be done by selective reinforcement of critical areas through spray deposition or some other route. In general, it is important for wear resistance to be combined with other properties such as high thermal conductivity and high stiffness (Ikechukwuka, 1997 and Rohatgi et al, 1988).

2.7.4 Corrosion Resistance

Galvanic corrosion is a major concern in AMCs. Crevice attack at the matrix/reinforcement interfaces and localized attack on structural and compositional in homogeneities can also occur within the matrix. Common reinforcements such as SiC, Al_2O_3 and graphite are nobler than the metallic matrices. In general the incorporation of these reinforcements increases corrosion rates of the metallic matrices, especially in the presence of air and chloride ions (Clyne, 2000 and Jokinen et al, 1992).

The corrosion resistance of AMCs is also strongly influenced by the conditions of fabrication and processing, which may lead to formation of an interphase between the matrix and reinforcement, interfacial stresses as well as high dislocation density in the matrix. The effect on corrosion of reinforcements appears to be also related to their geometry, volume fraction and electrical property. Generally particulates have corrosion resistance less than fibers, and the degradation is higher at higher volume fraction. As compared with SiC, Al_2O_3 has a lower tendency to enhance galvanic corrosion in AMCs since Al_2O_3 is an insulator (Clyne, 2000 and King, 1987).

The corrosion of AMCs can be reduced by anodizing or surface treatment. But the anodization is generally less effective on the composites in comparison with the unreinforced alloys. Insulating the reinforcements by coating the entire surface with suitable coatings can provide protection from corrosion (Maruyama, 1998).

2.8 EFFECT OF CERAMIC REINFORCEMENTS ON THE BEHAVIOR OF ALUMINIUM MATRIX IN AMCS

Presence of relatively large (more than 10%) volume fraction of ceramic reinforcement (whisker, particle, short fibre and continuous fibre) profoundly affect the behaviour of aluminium matrix in aluminium matrix composites during manufacturing, heat treatment and their subsequent use in service. These changes include both intrinsic and extrinsic ones (Surappa and Rohatgi, 1981, Sagail and Leisk, 1992).

2.8.1 Intrinsic Effects Ceramic Reinforcements

Intrinsic effects include microstructural changes, heat treatment characteristics and thermal stresses. These changes significantly alter and expand the physical, mechanical and tribological property limits of aluminium alloy (Clyne, 2000).

Presence of ceramic reinforcement can alter the solidification behavior of aluminium alloys in several alloys. Ceramic reinforcement can serve as a barrier to diffusion of heat and solute, catalyze the heterogeneous nucleation of phases crystallizing from the melt, restrict fluid convection, and induce morphological instabilities in the solid–liquid interface (Vogelsang et al, 1986).

Aluminium matrix composites often experience fabrication temperature in excess of 500^0C, and large thermal residual stresses are included on cooling. Magnitude of thermal residual stresses developed is related to many variables including the type of reinforcement, volume fraction, diameter and aspect ratio. For example, thermal residual stresses (tensile) of more than 100 MPa are present in the matrix of Al-30 vol% SiC particulates composites. Mechanical behaviour of AMCs is profoundly affected by thermal residual stresses. Presences of residual stresses caused by ceramic reinforcement

results in a symmetrical yielding, and also affect fatigue and creep behaviors of (Maruyama, 1998).

2.8.2 Extrinsic Effects of Ceramic Reinforcement

Incorporation of ceramic reinforcement in Aluminium alloys leads to significant improvement in the sliding wear resistance of AMCs as measured by the pin-on-disc set up against a hardened steel disc (Zhou and Xu, 1997).

In recent years extrinsic effect of SiC reinforcement in AMCs has been beneficially utilized in brake disc/brake pad tribocouple. When AMCs brake disc slides against brake pad adherent tribolayer are formed on the surface of AMCs disc at the contact region (Donne et al, 1990). Tribolayers thus formed, further enhances the wear resistance of the AMC discs. Tribolayers consisting of mixed oxides are formed due to transfer of material from the brake pad on to the AMCs disc during sliding (Surappa and Rohatgi, 1981, Clyne, 2000).

2.9 THERMAL TREATMENTS OF AMCs

2.9.1 Age Hardening Characteristics of Ceramic Reinforced Aluminium Alloys

The age hardening characteristics of an alloy are generally modified by the introduction of reinforcement. These modifications are due to the manufacturing process, the reactivity between the reinforcement and the matrix, the size, morphology and volume fraction of the reinforcement (Clyne, 2000 and Bayourni et al, 1988).

The size, morphology and volume fraction of the reinforcement, are factors controlling the plasticity and the thermal residual stresses in the matrix. The sink effect due to interfaces introduced by the presence of the reinforcement may also play an important role in precipitation kinetics. The manufacturing process may lead to different

microstructures, which would also modify the precipitation kinetics. The reactivity between the reinforcement and the matrix during the elaboration process and during the high temperature solution treatment may lead to a modification of the composition of the matrix.

Strength increment due to ageing is necessary in these alloys because it helps to develop acceptable mechanical properties. When heat-treating age-hardenable AMCs, it is often assumed that the composites heat-treats in a manner identical to the unreinforced aluminium alloy (Clyne, 2000 and Bayourni et al, 1988).

In AMCs fabricated by molten-metal methods, a ceramic reinforcement alters the ageing characteristics of the matrix of AMCs by depleting the precipitate-forming elements during the fabrication stage. The depletion is caused by chemical reactions between the matrix alloy and the reinforcement, a phenomenon that has been reported in many MMCs (Ribes et al, 1990; Lepetitcorps et al, 1991 and Lloyd et al, 1900). For instance, aluminum oxide, $A1_20_3$, is known to be stable in pure aluminium, but reacts with magnesium in Mg-containing aluminium alloys to form MgO and $MgA1_2O_4$ (spinel) as shown in the following equations:

$3Mg + Al_2O_3 = 3MgO + 2Al$ (ΔG = -117.4kJ at 1000K)

and $3Mg + 4Al_2O_3 = 3MgAl_2O_4 + 2Al$ (ΔG = -2 15.1kJ at 1000K)

MgO may form at high magnesium levels and lower temperatures whereas the spinel will form even at very low magnesium levels (Ikechukwuka, 1997). Therefore, it is not surprising that Al_2O_3 is not thermodynamically stable in most aluminum alloys.

Unlike SiC, which is stable below the solidus, alumina remains unstable in the solid state. Therefore, reactions may still take place during a normal solution heat

treatment operation or solid-state processing. Reinforcement reactions have been responsible for the presence of intermetallics such as $MgA1_2O_4$ spinel in the matrices of MMCs (Ribes et al, 1990 and Lepetitcorps et al, 1991).

Dislocation generation is another important effect associated with ceramic phase additions to metal alloys. When a metal matrix containing a ceramic reinforcement is cooled from the fabrication or solution heat treatment temperature, large tangles of dislocations are generated in the matrix alloy due to the difference between the coefficients of thermal expansion (CTEs) of the ceramic reinforcement and the matrix (Bayourni et al, 1998 and Vogelsang et al, 1986). The difference in CTEs gives rise to stresses usually large enough to deform the matrix plastically.

Dislocations are high-energy sites that facilitate the nucleation of strengthening phases in age-hardenable alloys. Transmission electron microscopy (TEM) studies have shown non-uniform distribution of dislocations in many MMCs (Vogelsang et al, 1986). Currently, three major hypotheses have been proposed to explain the small increase in hardness that occurs when discontinuously reinforced MMCs are aged artificially.

1) It has been attributed to the relatively small amount of solute atoms available for precipitation reaction in a reactive matrix (i.e.: a matrix in which one or more of the solute elements reacts with the reinforcement phase). In such instances, the amount of available solutes is found to decrease with increasing volume fraction of the reinforcing phase (Bayourni et al, 1998). Reduced hardening has been associated with acceleration of non-coherent precipitation reactions on dislocations and other high-energy sites (Bayourni et al, 1998 and Vogelsang et al, 1986).

2) Reinforcement-induced segregation and selective precipitation in the vicinity of the matrix-reinforcement interfaces have been reported in Al-Si-Mg/SiC, composites (Bayourni et al, 1998). Interfacial reaction and elemental segregation reduce the amount of precipitate-forming elements available for hardening. Many researchers have been carried out in the past to develop and improved aluminium base composites with the aim of achieving better mechanical properties (Clyne, 2000).

Dionne, et al (1990) studied the age-hardening behavior of a 30%vol SiC particle/A7091) composite and found that the ageing response was very rapid, in that order only one hour ageing at 120^{O}C, 45% of the peak tensile strength and 69% of the peak hardness were attained, compared to the unreinforced aluminium alloy.

Cottu, et al (1992) showed that the hardening kinetics of an AS 7G06A1 alloy/10%vol SiC fiber composite enhanced by the presence of the reinforcement during heat treatment. The authors explained this by the plastic deformation induced by the heat treatment due to the coefficient of thermal expansion (CTE) mismatch between matrix and reinforcement, as well as the highest dislocation density in the composite that supplied precipitation sites.

Srivetson and Mattingly (1993) also attributed the enhanced properties of heat-treated 2124 Al alloy/SiC fiber composites to CTE mismatch and higher dislocation density factor.

2.9.2 Principles of Age Hardening of Aluminium alloys

Heat treatment processes for increasing the strength and hardness of either wrought or cast aluminium alloys utilize the mechanism of precipitation hardening. One essential attribute of a precipitation hardening system is a temperature and time dependent equilibrium solid-solubility characterized by decreasing solubility with decreasing temperature and then followed by solid-state precipitation of second phase atoms on cooling in the solidus region. These conditions are usually met by most aluminium equilibrium systems of heat-treatable types (Rajan and Sharma, 1988). The first stage of precipitation can be made to occur at room temperature and this is called natural ageing while subsequent precipitations can be accelerated by heating the alloy to slightly above the room temperature and then cooling in air, which is referred to artificial ageing. Precipitation heat-treatment for the purpose of increasing strength and hardness is a three-step process. The first step is the solution heat-treatment that involves dissolution of soluble phases followed by quenching for the development of super-saturation and then ageing which is the precipitation of solute atoms either at room temperature (natural aging) or elevated temperatures (artificial ageing) (Markandeya et al, 2004, Rajan and Sharma, 1988).

In order to take the advantage of the precipitation hardening reaction, it is necessary first to produce a solid solution(solution heat-treatment). Production of a solid solution consists of soaking the aluminium alloy at a temperature sufficiently high and for such a time so as to attain an almost homogeneous solid solution. The soaking time is

required to achieve a satisfactory degree of dissolution of the undissolved or precipitated soluble phase constituents and for attainment of a reasonable degree of homogeneity (Rajan and Sharma, 1988).

Quenching is carried out to avoid slow cooling which may result in the precipitation of phases that may be detrimental to the mechanical properties or to the corrosion resistance of the alloys/composites. For these reasons solid solutions formed during solution heat-treatment are quenched rapidly in liquid without interruption to produce a supersaturated solution at room temperature (Markandeya et al, 2004).

After the formation of a super saturated solid solution then the precipitation of the solute atoms (ageing) followed which is usually accomplished naturally or artificially Precipitation heat-treating is used to impart high strength and hardness to aluminium alloys. Generally artificial ageing imparts higher strength and hardness values to aluminium alloys without sacrificing other mechanical properties and also improves the resistance of these alloys to exfoliation and stress- corrosion cracking (Rajan and Sharma, 1988, Gosh et al, 2004).

2.9.3 Kinetic Analysis of Precipitation Reactions

The mechanical properties of age-hardenable aluminum alloys are determined largely by chemical composition, manufacturing method and heat treatment. The improvement of mechanical properties by heat treatment is largely attributed to the formation of metastable phases during ageing (Rajan and Sharma, 1988).

The primary objective of kinetic analysis is to identify the kinetic equations controlling the precipitation process. There are a number of isothermal and non-isothermal techniques, which can be used to study the kinetics of precipitation processes

in metals and alloys. The techniques include electrical resistivity, differential scanning calorimetry (DSC), hardness measurements, dilatometry, and thermoelectric power (TEP) measurement. In general, TEP, resistivity, and hardness measurements are used to study the kinetics under isothermal conditions while DSC and dilatometry techniques are used for non-isothermal conditions.

Mittemeijer et, al (1998); Meisel and Cote (1983), Starink and van Mourik (1992) have used DSC, dilatometry, or both to study precipitation reactions in different metallic alloys and employed different versions of the Kissinger (1957) analysis to calculate the kinetic parameters. Kinetic parameters have been determined from hardness measurements. Arrhenius Analysis of ageing kinetics in aluminum-based AMCs has been carried out by Nieh and Karlak, (1984), Song and Baker, (1994). The validity of this method is based on the fact that Arrhenius analysis uses only the time to peak hardness and temperature of ageing rather than the absolute hardness values.

In this technique, it is assumed that:

1) Peak hardness corresponds to the same level of transformation in each case
2) Ageing temperatures are low enough for the transformation to be diffusion controlled.

Hence, the activation energy for diffusion can be calculated from the time to peak hardness. The Arrhenius equation for diffusion is given as :

$$D = D_0 \exp\left(\frac{-E}{RT}\right) \tag{9}$$

Where:

D = diffusion coefficient,

Do = material constant,

E = activation energy for diffusion (J/mol),

R = universal gas constant (8.34 J/mol K)

and T = absolute temperature (K).

The logarithmic form of equation is given as:

$$\text{InD} = \text{InDo} - \left(\frac{E}{R}\right)\frac{1}{T} \qquad (10)$$

When D is replaced with $In\frac{1}{t}$ (where t is the time to peak hardness) a plot of $In\frac{1}{t}$ against $\frac{1}{T}$ for a range of temperatures gives a straight line with slope $\frac{-E}{R}$ allowing the activation energy, *E,* to be calculated.

There is yet to be a consensus on the most appropriate mathematical recipe for the extraction of kinetic data from solid-state transformation experiments. There are objections in the literature against the use of the Kissinger analysis, which was originally derived for homogeneous reactions (e-g., gas phase chemical reactions), for the study of the generally heterogeneous solid-state transformations in metallic alloy. The three main objections are:

(i) Thermal gradients are inherent in non-isothermal methods. Therefore, it is claimed that significant inaccuracy will result from the application of the Kissinger analysis which does not allow for the presence of thermal gradients;

(ii) The order of reaction equation often assumed in the Kissinger method is appropriate for homogeneous transformations but not valid for the heterogeneous transformations which take place in solid-state reactions;

(iii) The reaction rate theory, which is considered appropriate only for isothermal experiments, is normally assumed in the Kissinger method (Mittemeijer et al, 1998; Meisel and Cote, 1983, Starink and van Mourik, 1992).

In all, the continued use of the activation energy-based analyses for describing nucleation, growth, and overall transformation kinetics in metals has been strongly criticized in the literature (Wendlandt et al, 1986). This is largely due to their tendency to produce meaningless and misleading results. It has been shown that when nucleation and growth occur simultaneously, the activation energy obtained from an Arrhenius-type plot for the rate data is the sum of the positive and negative energy values for nucleation and diffusion growth mechanisms. Nevertheless, due to what seems to be the Lack of a better quantitative method, experimental determinations of activation energies have continued to be used for describing the kinetics of phase transformations in metals.

2.10 APPLICATIONS OF AMCS

AMCs now have a proven track record as successful "high-tech" materials in a range of applications. AMCs utilizations provide significant benefits including performance benefits (component lifetime, improved productivity), economic benefits (energy savings or lower maintenance cost) and environmental benefits (lower noise levels and fewer air-borne emissions). Engineering viability of AMCs in a number of applications has been well documented. AMCs having different type of reinforcements (whiskers, particles, short fibres and continuous fibres) have been produced both by solid state and liquid state processing (Surappa and Rohatgi, 1981, Ikechukwuka, 1997). Among the various and numerous applications, are mentioned below and shown in Figure 2.2.

Brake rotors for German high-speed train ICE-1 and ICE-2 developed by Knorr Bremse AG and made from a particulate reinforced aluminum alloy (AlSi7Mg+SiC particulates) supplied by Duralcan. Compared to conventional parts made out of cast iron with 120 kg/piece, the 76 kg of the AMC rotor offers an attractive weight saving potential

The braking systems (discs, drums, calipers or back-plate) of the New Lupo from Volkswagen was made from particulate reinforced aluminum alloy supplied by Duralcan.

AMCs continuous fiber reinforced pushrods produced by Duralcan for racing engines. These pushrods weigh 40% as much as steel, they are stronger and stiffer, and have high vibration damping. AMCs wires also developed by Duralcan for the core of electrical conductors. The unique properties of this type of conductor offer substantial performance benefits when compared to the currently used steel wire reinforced conductors.

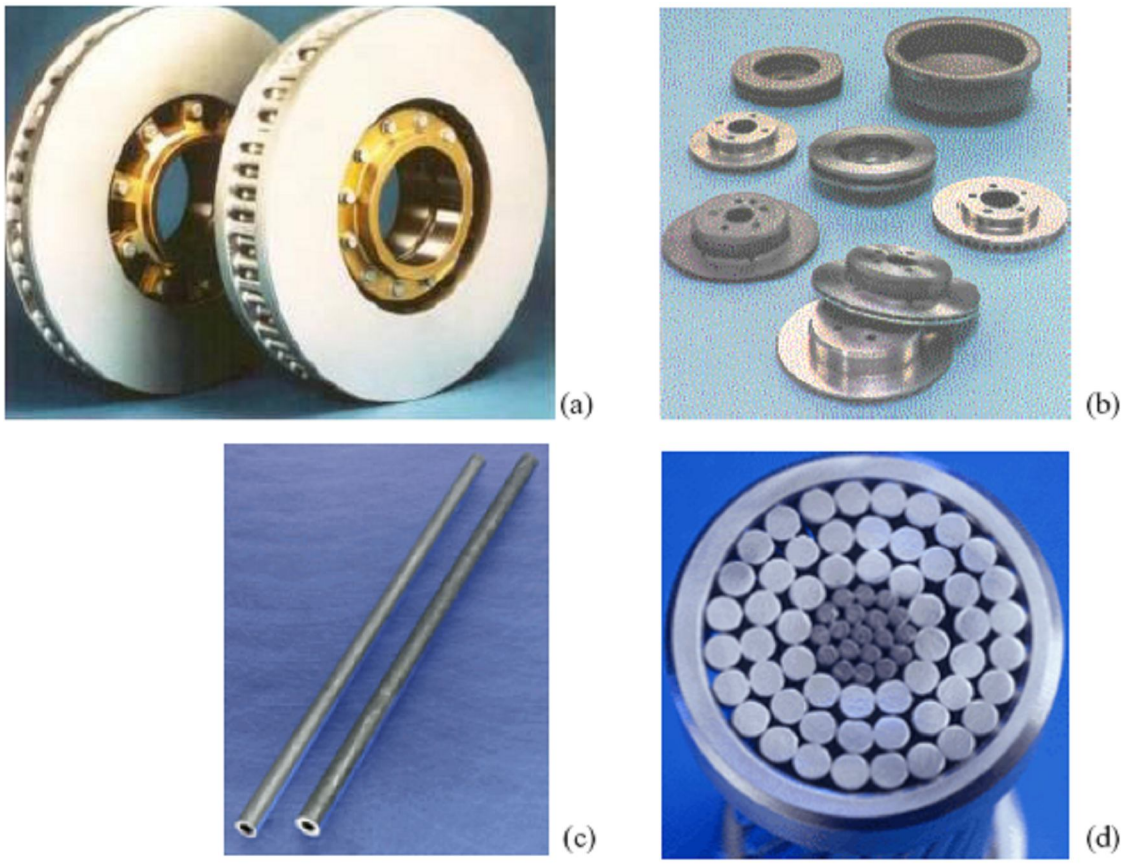


Figure 2.2: Some Industrial Applications of AMCs (a) brake rotors for high speed train (b) automotive braking systems (c) automotive pushrods (d) cores for HV electrical wires

Sources: Surappa et al, 1981 and Ikechukwuka, 1997.

CHAPTER THREE

3.0 MATERIALS AND METHODS

The materials and experimental methods employed in this research work are explain below,

3.1 MATERIALS

The materials used in this study are: Silicon carbide with average particle size of 10μm, Ferrosilicon, high purity aluminium electrical wire which was obtained from Northern Cable Company NOCACO (Kaduna)(see plate C1) Appendix C. Moulding boxes, Silica sand, Bentonite were obtained from the Foundry Shop of National Metallurgical Development Centre, Jos, Nigeria.

3.2 EQUIPMENT

The equipment used in this study included: Pyrometer, mechanical stirrer, crucible, electrical resistance furnace, Rockwell hardness tester, Charpy impact machine, Tinus Olsen tensile machine and Metallurgical microscope with built-in camera.

3.3 METHODS

3.3.1 Samples Production

The synthesis of the metal matrix composite that was used in this study was produced using double stir-casting method at the Foundry Shop of the National Metallurgical Development Center, Jos, Nigeria. The samples were produced by keeping the percentage of iron and silicon constant and varying the Silicon carbide particles in the range 5-25wt%. High purity aluminium electrical wires was charged in a graphite

crucible kept in an electric resistance furnace and 0.01%NaCl-KCl powder was used as a cover for melting the alloy in order to minimize oxidation of aluminium by excluding oxygen and creating a protective atmosphere inside the furnace. After the melting of pure aluminium, the temperature of the furnace was raised to 720^{o}C for the purpose of superheating the aluminium melt. The required quantity of 2.8% silicon and 0.8%iron was added to the melt using ferrosilicon, and the melt was thoroughly stirred.

With progressive melting, the furnace temperature was raised to 780^{O}C and the melt was held at this temperature for 10 minutes. It was then skimmed to remove the oxides and impurities. The molten metal was continuously stirred in order to ensure a near-uniform distribution of alloying elements and prevent the elements from settling at the bottom due to their higher density. For each melting, 400g of charge materials was used to produce the alloy. Silicon carbide particles, were preheated to 1000^{O}C, to make their surface oxidized.

The alloy was then cooled down to temperature just below the liquidus point(580^{o}C)to keep the slurry in a semi-solid state. At this stage the preheated SiC particles was added and mixed manually. Manual mixing was used because it was very difficult to mix using automatic device when the alloy was in a semi-solid state. After manual mixing was done, the composite slurry was re-heated to a temperature of 720^{O}C and then automatic mechanical mixing was carried out for about 20 minutes at an average stirring speed of 150 rpm. In the final mixing processes, the furnace temperature was controlled between 730 and 740^{o}C and the pouring temperature were controlled to be about 720^{o}C.

A preheated sand mould with diameter 18 mm *and* 300mm length was used to produce cast bars (see plate C2) Appendix C. After casting, the density and porosity of the varying composition produced were determined and the samples were machined into tensile, impact and hardness test specimens for the purpose of determining the mechanical properties.

3.3.2 Heat Treatment of the Samples

The test samples were solution heat-treated at temperature of 500^{o}C in an electrically heated furnace, soaked for 3 hours at this temperature and then rapidly quenched in warm water at 65^{o}C. Ageing of the test samples were carried out at temperatures of 100, 200 and 300^{o}C, for various ageing times of 60 to 660minutes, and then cooled in air. The ageing characteristic of these grades of composites was evaluated using hardness values obtained from solution heat-treated samples of the investigated composites subjected to the aforementioned temperature conditions. The tensile and impact tests were conducted at peak ageing time of the various ageing temperatures.

3.3.3 Determination of Density

The basic method of determining the density of a specimen is by measuring the mass and volume of the sample used. The density of the sample was then estimated from equation (1):

3.3.4 Determination Apparent Porosity

The basic method of determining the apparent porosity of aluminium alloy was used in determining the apparent porosity of the as-cast and aged hardened Al-Si-Fe/SiC composites. The apparent porosity of the sample was then estimated from equation (2)

3.3.5 Hardness Values Determination

The hardness values of both as-cast and age-hardened samples were determined according to the provisions in ASTM E18-79 using the Rockwell hardness tester on "B" scale (Frank Welltest Rockwell Hardness Tester, model 38506) with 1.56mm steel ball indenter, minor load of 10kg, major load of 100kg and hardness value of 101.2HRB as the standard block. Before the test, the mating surface of the indenter, plunger rod and test samples were thoroughly clean by removing dirt, scratches and oil and calibration of the testing machine using the standard block. The samples were placed on anvils, which act as a support for the test samples. A minor load of 10kg was applied to the sample in a controlled manner without inducing impact or vibration and zero datum position was established, and then the major load of 100kg was then applied, the reading was taken when the large pointer came to rest or had slowed appreciably and dwelled for up to 2 seconds. The load was then removed by returning the crank handle to the latched position and the hardness value read directly from the semi automatic digital scale (Metal handbook, 1985).

3.3.6 Determination of the Tensile properties

The tensile properties of the as cast and peaking ageing samples were conducted on Tinus– Olsen testing machine. The test pieces were machined to the standard shape and dimensions as specified by the American Society for testing and Materials (Annual books of ASTM standard, 1990). The sample was locked securely in the grips of the upper and lower crossbeams of the testing machine. A small load was initially applied to seat the sample in the grips and then the load was increased until failure occurred.

3.3.7 Impact Strength Determination

The impact test of the as cast and peaking ageing samples for was conducted using a fully instrumented Avery Denison test machine. The mass of the hammer was 22 7 kg and the striking velocity was 3.5 m/sec. Charpy impact tests were conducted on notched samples. Standard cylinder impact test sample measuring 75 x 10 x 10 mm with notch depth of 2 mm and a notch tip radius of 0. 02 mm at angle of 45^{o} was used.

Before the test sample was mounted on the machine, the pendulum was released to calibrate the machine. The test samples were then gripped horizontally in a vice and the force required to break the bar was released from the freely swinging pendulum. The value of the angle through which the pendulum has swung before the test sample was broken corresponded with the value of the energy absorbed in breaking the sample and this was read from the calibrated scale on the machine (Metal handbook, 1985).

3.3.8 Microstructural Examination

Metallographic specimens were cut from the as-cast and age-hardened samples of the Al-Si-Fe/SiC particulate composite. The cut samples were mounted in Bakelite, and mechanically ground progressively on grades of SiC impregnated emery paper (80-600 grits) sizes using water as the coolant. The ground samples were polished using one-micron size alumina polishing powder suspended in distilled water. Final polishing was achieved using 0.5-micron alumina polishing powder suspended in distilled water. Following the polishing operation, etching of the polished sample was done using Keller's reagent. The microstructure obtained was photographically recorded using an optical microscope with built-in camera.

CHAPTER FOUR

4.0 RESULTS AND DISCUSSION

4.1 PHYSICAL PROPERTIES OF Al-Si-Fe/SiC COMPOSITES

4.1.1 Macrostructural Analysis

Macrostructural studies of the cast composites before and after machining revealed a reasonably uniform distribution of SiC particles and a slight macro-segregation of particles in some places. The distribution of SiC particles is influenced by good wettability of the silicon carbide by the molten metal and good interfacial bonding between SiC particles and matrix material (see Plates C3-C4) in Appendix C.

4. 1.2 Density

The result of density measurements on the base alloy and reinforced materials are shown in Table 4.1and Figure B1 (Appendix B).

Table 4.1: Density of Al-Si-Fe Alloy with Percentage of Silicon carbide

wt% SiC	Weight(grams)	Volume(cm^3)	Density(g/cm^3)
0	22.220	8.00	2.78
5	16.521	6.00	2.75
10	18.944	7.00	2.71
15	19.010	7.0	2.72
20	19.784	7.50	2.64
25	18.714	7.50	2.50

The results reveal that the presence of SiC particulates has little effect on the density of the AMCs. Since the density of the reinforced SiC particles composites decreased from 2.75 g/ cm^3 at 5wt% of SiC addition to 2.50 g/ cm^3 at 25 wt% of SiC addition. Hence, not much change in the AMCs density was observed. This work is in

line with the earlier work carried out by Ramachandra and Radhakrisha (2006), who also found out that the density of reinforced alloy with 25%SiC is 2580Kg/mm^3 and that of unreinforced aluminium alloy 2630Kg/mm^3.

4.1.3 Apparent Porosity

Table 4.2 and Figure B2 (Appendix B) show the results of apparent porosity of the base Al-Si-Fe alloy and reinforced materials.

Table 4.2: Apparent Porosity of Al-Si-Fe Alloy with Percentage of Silicon Carbide

wt% SiC	W_1 grams	W_2 grams	W_3 grams	$P_a = \frac{W_3 - W_1}{W_3 - W_2} x100(\%)$
0	19.0188	11.9560	19.0279	0.13
5	16.5223	10.3948	16.5333	0.18
10	22.2315	13.9718	22.2519	0.25
15	19.7806	12.2947	19.8034	0.30
20	18.7171	11.7670	18.7408	0.34
25	18.9400	11.7213	18.9707	0.42

The apparent porosity values of the reinforced AMCs with SiC particles slightly increased with percentage SiC additions (see Table 4.2) and Figure B2 (Appendix B). The apparent porosity increased from 0.13% to 0.43% for the Al-Si-Fe alloy and alloy reinforced with 25wt% SiC respectively. These values were lower than that obtained by other researchers which range from 2-4% (Rohatgi et al, 1988; Zhou and Xu, 1997, Whitehouse et al, 1991). The lower values of apparent porosity obtained in this study were as a result of the use of a covering fluxes combined with double stirring method during casting. This prevented the composites slurries from oxidation and also

breakdown the gas layer. This made the particles sink to the bottom due to higher specific weight rather than float to the surface and this enhanced good wettability.

4.2 KINETIC CHARACTERISTICS OF AGEING

Arrhenius analysis of ageing kinetics in aluminum-based metal matrix composites (MMCs) was used to determine the kinetics parameters (Kissinger, 1957; Nieh and Karlak, 1984, Song and Baker, 1994). The value of the activation energy was estimated using equations (9-10).

The activation energy for diffusion E, of the ageing process is tabulated in Table 4.3 and shown in Figures B3-B4 (Appendix B)

Table 4.3: Kinetics Analysis of Al-Si-Fe Alloy with Percentage of Silicon Carbide

% of SiC addition	Time to Peak aged at 100^{O}C Minutes	Time to Peak aged at 200^{O}C Minutes	Time to Peak aged at 300^{O}C Minutes	Activation energy of diffusion J/mol
0	540	420	420	2241.94
5	480	300	240	6187.74
10	420	300	240	5021.94
15	360	240	180	6187.94
20	360	240	120	9864.52
25	300	180	60	14438.07

The acceleration to precipitation(R) was measured by the ratio $R = \frac{tpHc}{tpHm}$ of times corresponding to peak hardness in the composite and to peak hardness in the unreinforced Al-Si-Fe matrix. The result is shown in Table 4.4 and Figure B5 (Appendix B).

Table 4.4: Acceleration to Precipitation Hardening(R) of Al-Si-Fe Alloy with Percentage of Silicon Carbide

% wt of SiC addition	Peak ageing time(hours) at $100^{O}C$	Acceleration to precipitation hardening(R)
0	10	----
5	9	0.900
10	8	0.800
15	7	0.700
20	7	0.700
25	6	0.600
% wt of SiC addition	Peak ageing time(hours) at$200^{O}C$	Acceleration to precipitation hardening(R)
0	8	-----
5	6	0.750
10	6	0.750
15	5	0.625
20	5	0.625
25	4	0.500
% wt of SiC addition	Peak ageing time(hours) at$300^{O}C$	Acceleration to precipitation hardening(R)
0	8	------
5	5	0.625
10	5	0.625
15	4	0.500
20	3	0.375
25	2	0.250

Table 4.3, shows that the activation energy of diffusion increases with increasing weight fraction of the silicon carbide in the alloy. Thus, an increase in volume fraction of the reinforcing particles accelerates the ageing kinetics, bringing about observable increase in hardness and concurrent decrease in ageing time (see Table 4.4), since the values of acceleration to precipitation obtained is less than one.

The ageing response measured by the variation of hardness with time of the composites for all five-volume fractions of the silicon carbide-reinforcing phase in the metal-matrix are shown in Table 4.5-4.7 and presented in Figures B6-B8 (Appendix

Table 4.5: Hardness (HRB) Characteristics at 100^{O}C with Percentage of Silicon Carbide

%wt SiC	0 minute	60 minutes	120 minutes	180 minutes	240 minutes	300 Minutes	360 minutes	420 minutes	480 minutes	540 minutes	600 minutes	660 minutes
0	38.0	39.5	40.5	45.0	48.0	50.6	52.5	56.5	57.0	58.0	60.1	58.0
5	58.0	58.0	59.0	60.0	62.0	62.0	63.0	67.0	68.5	70.3	72.0	70.0
10	59.5	61.0	63.0	65.0	67.0	69.0	73.0	73.0	75.0	73.0	70.0	76.0
15	64.8	65.0	65.5	67.0	70.0	73.0	79.0	82.0	76.0	73.0	69.5	66.0
20	68.8	69.0	70.0	71.5	74.0	79.0	82.0	86.0	77.0	72.0	70.0	65.0
25	71.5	72.0	72.0	74.0	78.0	84.0	89.5	81.0	76.0	74.0	70.0	64.0

Table 4.6: Hardness (HRB) Characteristics at 200^{O}C with Percentage of Silicon Carbide

%wt SiC	0 minute	60 minutes	120 minutes	180 minutes	240 minutes	300 minutes	360 minutes	420 minutes	480 minutes	540 minutes	600 minutes	660 minutes
0	44.5	45.0	47.0	50.1	55.0	57.0	60.0	60.2	61.5	58.0	48.0	40.5
5	65.0	65.0	68.0	69.0	69.5	71.0	73.0	70.0	67.0	62.0	60.0	59.0
10	65.8	67.0	69.0	70.0	72.0	73.0	74.5	71.0	68.0	68.0	64.5	60.0
15	67.9	69.0	69.0	76.6	77.5	84.0	75.0	71.2	70.0	67.0	65.1	63.0
20	71.3	73.0	74.5	75.0	80.0	87.0	76.0	72.0	69.5	66.5	66.0	64.0
25	75.0	75.0	80.0	85.0	89.0	78.0	74.0	70.0	68.0	67.0	64.0	62.0

Table 4.7: Hardness (HRB) Characteristics at 300^{O}C with Percentage of Silicon Carbide

%wt SiC	0 minute	60 minutes	120 minutes	180 minutes	240 minutes	300 minutes	360 minutes	420 minutes	480 minutes	540 minutes	600 minutes	660 minutes
0	45.0	46.0	50.5	52.0	58.0	60.0	60.1	61.0	62.0	56.0	55.0	52.0
5	66.4	68.0	70.0	72.0	72.5	74.0	67.0	65.0	64.0	64.0	62.0	61.0
10	68.9	70.0	79.0	80.0	82.0	84.0	73.0	69.0	65.0	64.0	61.0	60.0
15	75.0	75.0	79.0	81.0	82.0	85.0	73.5	69.0	65.0	64.0	63.5	62.0
20	78.5	79.0	82.0	89.0	83.0	70.0	65.0	64.0	62.0	62.0	60.0	58.0
25	81.3	84.5	90.5	88.0	75.0	69.0	66.0	65.0	64.0	62.0	60.0	56.0

From these tables, it can be seen that there is steep rise in hardness values of each grade of the composite at initial stages for all ageing temperatures and then fell after reaching the various peak ageing time and the hardness values decreases, corresponding to over ageing. However, at higher ageing temperature the materials develop peak hardness at shorter ageing time, because the rate of precipitation of the second phase materials is faster and hence increases in hardness values. The time to obtain peak hardness is shorter according to the sequence: $100^{O}C > 200^{O}C > 300^{O}C$ (see Table 4.4) and Figure B9 (Appendix B).

The age hardening behavior of the Al-Si-Fe/SiC particulates composites are similar to Al-Si-Mg/5%SiC particulates as reported by Cottu, et, al (1992) i.e. hardness continuously increases to a maximum during ageing and them decreases later due to over ageing. It is interesting to note that in the reinforced aluminium alloy metal-matrix, as the volume fraction of SiC in the aluminium alloy metal-matrix increases there is a monotonic reduction in the time required to reach peak hardness (see Table 4.4).

4. 2.1 Statistical Analysis of the Ageing Process

Two levels of each of the three factors were used for the statistical analysis. The levels for the three factors are entered in Table 4.8 and the treatment combinations for the two levels and these three factors are tabulated in Table 4.9.

Table 4.8: Statistical Design Of the Ageing Process

Factors	Low level	High level
Temperature (X)	$100^{O}C$	$300^{O}C$
%wt of SiC(Y)	5.0	25.0
Time(Z)	60minutes	660minutes

Table 4.9: Factorial Design of the Ageing Process Showing Treatment Combination

Exp.number	Temperature level	%wt of SiC level	Time level
1	Low	Low	Low
X	High	Low	Low
Y	Low	High	Low
Xy	High	High	Low
Z	Low	Low	High
Xz	High	Low	High
Yz	Low	High	High
Xyz	High	High	High

The results and treatment conditions are shown in Table 4.10.

Table 4.10: Experimental Conditions and Hardness Values for each given Condition

Exp.combination	Temperatures	%wt SiC	Time (Minutes)	Hardness values(HRB)
1	100^{O} C	5	60	58.0
X	300^{O} C	5	60	68.0
Y	100^{O} C	25	60	72.0
Xy	300^{O} C	25	60	84.5
Z	100^{O} C	5	660	68.0
Xz	300^{O} C	5	660	61.0
Yz	100^{O} C	25	660	64.0
Xyz	300^{O} C	25	660	56.0

The Yates analysis was used to determine the main effects and interaction of the Factor

Table 4.11, give the Yates table.

Table 4.11: Yates Analysis Table

Treatment combination	Hardness values(HRB)	Column 3	Column 4	Column 5	Mean effect	Treatment combination
(1)	58.0	58+68= 126	126+156.5=282 .5	282.5+248=530 .5		
X	68.0	72+84.5=156. 5	128+120= 248	-15+20=5	5/4=1.25	Temperature
Y	72.0	68+61= 128	10+10=20	-8+30.5= 22.5	22.5/4= 5.63	% wt of SiC
Xy	84.5	64+56= 120	-8+-7=-15	-1+0=-1	-1/4= -0.25	Temperature & %wt SiC
Z	68.0	68-58=10	156.5-126= 30.5	248-282.5= -34.5	-34.5/4= -8.63	Time
Xz	61.0	84.5-72= 10	120-128=-8	-15-20= -35	-35/4= -8.75	Temperature & Time
Yz	64.0	61-68=-7	10-10=0	-8-30.5= -38.5	-38.5/4= -9.63	%wt SiC & Time
Xyz	56.0	56-64=-8	-8—7=-1	-1-0=-1	-1/4= -0.25	Temperature, %wt SiC & Time

The sum of squares is obtained by squaring the values in the 5th column of the Yates table

and dividing by the number of observations (8 in this case). The variance ratio is = Means – Square / Error – Square . The values of the variance ratio are given in Table 4.12 (Irwin and Freund, 1987).

Table 4.12: Analysis Of Variance of the Effects

Source of variation	Sum of squares	Degrees of freedom	Mean squares Variance ratio	
Main effects:				
Temperature %wt of SiC Time	3.125 63.28 148.78	1 1 1	3.127 63.28 148.78	0.037 0.78 1.76
Interactions:				
Temperature & %wt of SiC Temperature & time %wt of SiC & Time Temperature, %wt of SiC & Time	0.125 153.13 185.28 0.125	1) 1) 1)total interactions =4 1)	84.67	

From the result of factorial design, the %wt of SiC appears to be the most important variable with main effect of 5.63HRB followed by temperature with 1.25HRB and time -8.63HRB. The analysis shows that raising the temperature from 100 to 300^{o}C would result in increase in hardness values by 1.25HRB, while allowing ageing to continue from 60 to 660 minutes would result in decreased hardness values by 8.63HRB and increasing the %wt of SiC from 5 to 25 would result in increasing the hardness values by 5.63HRB.

The estimated interactions between temperature and %wt of SiC; temperature and time; %wt of SiC and time and then between the three factors temperature; %wt of SiC and time are -0.25HRB, -8.75HRB, -9.63HRB and -0.25HRB respectively. This means that raising temperature and time would result in decrease in hardness values by

8.75HRB whereas raising all the three factors would result in decrease in hardness values by 0.25HRB. From the results of statistical analysis, %wt of SiC and time are the most important parameter in the ageing of Al-Si-Fe/SiC particulate composites.

4.3 MICROSTRUCTURAL ANALYSIS

Microstructures of the as-cast and heat-treated composites at various ageing temperatures and peaking ageing time were examined by the used of metallurgical microscope. They were observed to contain primarily α-Al, silicon eutectic and SiC particles as shown micrographs A4.1-A4.24 (Appendix A). In the microstructure of the composites Si phase was seen apparently in the eutectic regions, and intermetallic compounds such as $FeSiAl_3$, iron-containing phases due to the secondary alloying elements.

The microstructure of the as-cast unreinforced Al-Si-Fe alloy is shown in micrograph A4.1 (Appendix A), while Micrographs A4.2-A4.6(Appendix A) show the microstructure of the as-cast reinforced alloy with SiC particle.

The microstructure reveals that there are small discontinuities and a reasonably uniform distribution of SiC particles. The ceramic phase is shown as dark phase, while the metal phase is white. However, there an agglomeration and segregation of SiC particles in the micro scale with alloy reinforced with 25% SiC particle (see micrograph A6). These structures are in agreement with the co-continuous interlaced phases studied by other researchers (Rohatgi et al, 1988; Zhou and Xu, 1997, Whitehouse et al, 1991). Micrographs A7-A.24(Appendix A) show the microstructure of the age-hardened Al-Si-Fe/SiC composites. The microstructure reveals the dissolution and distribution of the SiC

particle in the metal matrix and present of precipitates at the particles matrix interfaces with precipitation and dissolution of the SiC particles and silicon eutectic phase.

The formation and presence of precipitates at the particles– matrix interfaces may be appreciated by comparing micrographs of the composite in the as-cast state micrographs (A1-A6) and in the peak age-hardened state micrographs (A7-A24) (Appendix A). The micrographs in the peak age-hardened state reveal precipitates covering the surface at the particles– matrix interfaces. Cottu et al, (1992) reported similar behavior of increased precipitation at interfaces for aluminum alloy 6061 reinforced with whiskers of silicon carbide.

4.4 MECHANICAL PROPERTIES OF Al-Si-Fe/SiC COMPOSITES

4.4.1 Hardness Values

Table 4.13 and Figure B10 (Appendix B) show the hardness values of both the as-cast and age-hardened Al-Si-Fe/SiC composites. From the figure, the hardness values for as-cast and age-hardened composite samples increases as the percentage Silicon carbide addition increases in the alloy. This is due to increase in the percentage of the hard and brittle phase of the ceramics body in the alloy.

Table 4.13: Hardness (HRB) For As Cast and Aged Hardened With Percentage of Silicon Carbide

wt% SiC	As-cast	Peak aged at $100^{O}C$	Peak aged at $200^{O}C$	Peak aged at $300^{O}C$
0	31.1	60.1	61.5	62.0
5	54.5	72.0	73.0	74.0
10	57.5	75.0	74.5	84.0
15	64.3	82.0	84.0	85.0
20	67.0	86.0	87.0	89.0
25	71.0	89.5	89.0	90.5

In comparison with the unreinforced Al-Si-Fe alloy, a substantial improvement in hardness was obtained in the reinforced metal matrices. It is noteworthy that in the

reinforced aluminium alloy metal-matrix, as the volume fraction of silicon carbide in the aluminium alloy metal-matrix increases, there is a monotonic reduction in the time required to reach peak hardness. With 5%wt of SiC addition, the samples exhibited a maximum hardness value of 72.0HRB at 100^{o}C for 9hours, 73.0HRB at 200^{o}C for 6hours and 74.0HRB at 300^{o}C for 5hours, while at 15%wt of SiC addition the samples have maximum hardness value of 82.0HRB at 100^{o}C for 9hours, 84.0HRB at 200^{o}C for 6hours and 85.0HRB at 300^{o}C for 5hours (see Figures B6-B8) (Appendix B).

The hardness values of the age-hardened alloy are almost equal at various ageing temperatures with percentage SiC additions (see Table 4.13). This is because the peak hardness has been obtained at the materials at these various ageing temperatures, which is also in line with earlier observation of Vogelsang et al (1986); Cottu et al (1992) and Ikechukwuka (1997).

4.4.2 Yield and Tensile Strength

The results of yield strength and ultimate tensile strength with weight fraction of Silicon carbide at various ageing temperatures are shown in Tables 4.14-4.15 and Figures B11-B12 (Appendix B).

Table 4.14: Yield Strength of Al-Si-Fe/SiC Composites with Percentage Silicon Carbide

wt% SiC	As-cast (N/mm^2)	Peak aged at 100^{O}C (N/mm^2)	Peak aged at 200^{O}C (N/mm^2)	Peak aged at 300^{O}C (N/mm^2)
0	45.60	59.90	56.40	52.40
5	57.57	65.20	64.80	63.00
10	68.46	73.35	75.00	73.00
15	72.38	78.0	78.91	74.00
20	79.98	80.75	82.50	80.34
25	70.50	72.90	75.60	74.80

Table 4.15: Tensile Strength of Al-Si-Fe/SiC Composites with Percentage Silicon Carbide

wt % SiC	As-cast (N/mm^2)	Peak aged at 100^OC (N/mm^2)	Peak aged at 200^OC (N/mm^2)	Peak aged at 300^OC (N/mm^2)
0	58.69	62.50	67.18	64.20
5	73.35	80.75	79.50	76.80
10	96.06	98.50	96.50	100.20
15	105.20	115.67	118.96	117.2
20	106.12	120.43	125.00	121.85
25	95.79	97.80	100.20	96.40

From tables 4.14-4.15, the yield strength and ultimate tensile strength of both the as-cast and age-hardened composites increased with increasing percentage Silicon carbide addition to maximum of 20 wt% SiC. The as-cast samples have a maximum value of 79.98 and 106.12N/mm^2 for yield and Tensile strength at 20% SiC addition and than decreased to 70.50 and 95.79 N/mm^2 for yield and Tensile strength at 25%SiC addition respectively.

For the age-hardened samples similar trend were also observed as for the case of the as-cast samples, in that the yield strength and ultimate tensile strength increased to a maximum values at 20% wt of SiC addition and then decreased beyond this point. The ultimate tensile strengths of the age-hardened samples at 20 wt% SiC are 120.43, 125.00 and 121.85N/mm^2 and at 25 wt% SiC addition are 97.80, 100.00 and 96.40N/mm^2 at peak ageing at 100, 200 and 300^OC respectively (see Figure B12)(Appendix B). Also the yield strengths of age-hardened samples at 20 wt% SiC addition are 80.75, 82.50 and 80.34N/mm^2, and that at 25 wt% of SiC addition are 72.90, 75.60 and 74.80N/mm^2 at peak ageing at 100, 200 and 300^OC respectively (see Figure B11)(Appendix B).

The higher values of both ultimate tensile strength and yield strength obtained at 20 wt% SiC than 25 wt% SiC are attributed to the uniform distribution of the SiC particles in the microstructure of the 20 wt% SiC (see Micrographs A5 and A4.19-A4.21) (Appendix A) than the microstructure of 25 wt% SiC (see Micrographs A6 and A22-A24) (Appendix A), it can be seen that the inter-atomic spacing in later is larger than in the former. The contribution of inter-atomic spacing to strain hardening arises from the fact that the space permitted a dislocation to maneuver round obstacles limit the yield stress given by the formula:

$\tau = \frac{Gb}{\lambda}$ (Dieter, 1988). τ= Yield stress, λ= Inter-particle spacing, G= Shear energy of dislocation and b= Burger vector.

The smaller the values of λ the greater the yield stress as a result of strain hardening. It therefore supports the fact that (micrographs A5 and A19-A21) (Appendix A) with smaller λ have greater strengths than (micrographs A6 and A22-A24) (Appendix A) with larger λ

When comparing these results with that of as-cast samples a substantial increase in both the yield strength and ultimate tensile strength was obtained. For example yield strength of Al-Si-Fe/5SiC particles increased from 57.57 to 64.80N/mm^2, ultimate tensile strength increased from 73.35 to 79.50N/mm^2 in the as-cast and peak age-hardened respectively. The yield and tensile strength of Al-Si-Fe/15SiC particles also increased from 72.38 to 78.91 N/mm^2 and 105.20 to 118.96 N/mm^2 in the as cast and age-hardened

at 200^{O}C temperature (see Tables 4.14-4.15).

These results show that Al-Si-Fe/5SiC particles samples has 8.38% and 12.56% increases in yield strength and ultimate tensile strength respectively over that of the as-cast samples at peak ageing at 200^{O}C, while for the Al-Si-Fe/15SiC particles the respective increments were 13.08% and 7.76% for yield strength and ultimate tensile strength. The increase in strength of the age-hardened samples over that of the as-cast are attributed to the uniform distribution of SiC in the aged samples than the as-cast samples (see Micrographs 4.2 and 4.11) and (Micrographs 4.4 and 4.17) respectively.

Sagail and Leisk (1992); Donne et al (1990) and Whitehouse et al (1991) attributed this to increase in dislocation density at interfaces. Increase in dislocation density strain hardens the metal-matrix locally and provides heterogeneous nucleation sites for precipitation, thereby accelerating the ageing response these modulated structure formed during ageing in all grade of composites enhanced this properties and is in agreement with the earlier works on Al-Si-Mg/SiC (Ikechukwuka, 1997 and Cottu et al, 1992).

4.4.3 Percentage Elongation

The results of percentage elongation with weight fraction of SiC at various ageing temperatures are shown in Table 4.16 and Figure B13 (Appendix B).

Table 4.16: Percentage Elongation of Al-Si-Fe/SiC Composites with Percentage Silicon Carbide

wt% SiC	As-cast	Peak aged at 100^{O}C	Peak aged at 200^{O}C	Peak aged at 300^{O}C
0	6.00	13.00	12.00	10.80
5	5.50	10.40	9.00	9.80
10	3.40	7.00	7.00	6.80
15	3.00	4.40	4.44	4.40
20	2.60	4.40	4.20	4.20
25	1.50	4.00	3.90	3.00

From table 4.16 and figure B13(Appendix B), it was observed that percentage elongation and percentage decreased as the percent Silicon carbide additions increases in the Al-Si-Fe alloy due to the addition of hard and brittle second phase (SiC) particles in the alloy. These results are in agreement with the work of other researchers (Clyne, 2000; Donne et al, 1990, Sagail and Leisk, 1992, Asthana, 1998).

4.4. 4 Impact Energy

The results of impact energy with weight fraction of Silicon carbide(SiC) at various ageing temperatures are shown in table 4.17 and figure B14 (Appendix B).

Table 4.17: Impact Energy For As Cast and Aged Hardened With Percentage of Silicon Carbide

wt% SiC	As-cast	Peak aged at $100^{O}C$	Peak aged at $200^{O}C$	Peak aged at $300^{O}C$
0	17.0J	28.0J	24.0J	22.0J
5	17.0J	26.0J	20.0J	20.0J
10	14.5J	20.0J	19.0J	19.0J
15	13.0J	17.5J	18.0J	18.0J
20	12.0J	17.0J	15.5J	16.0J
25	12.0J	16.0J	15.0J	14.0J

From the figure above, the impact energy of both the as-cast and age-hardened samples, decreased as the percent SiC addition increases in the alloy. The brittle nature of the reinforcing materials (SiC) plays a significant role in degrading the impact energy of the composite, since the unreinforced alloy and the alloy with 5% SiC particles have the highest impact energy, indicating that they are the toughest of them all.

CHAPTER FIVE

5.0 CONCLUSION AND RECOMMENDATION

5.1 CONCLUSION

In the present research, different experimental techniques have been used to characterize the microstructure and properties of Al-Si-Fe alloy and its composites containing different volume fractions of SiC particles. The metal matrix composites studied contained 5 – 25wt% of SiC particles. The evaluation of the microstructure and properties of the test samples were carried out using metallurgical microscopy, Rockwell hardness testing machine, Charpy impact test, Tinus Olsen tensile machine and statistical analysis.

From the results of the investigations and discussions in the preceding chapter, the following conclusion has been made.

1) The uniform distribution of the SiC particles in the microstructure of both the as - cast and age-hardened Al-Si-Fe/SiC composites is the major factor responsible for the improvement in the mechanical properties.
2) The good and better interfacial bonding between the alloy and the SiC particles resulted in the lower values of porosity obtained when using the double stir casting method.
3) There is not much, difference between the density of unreinforced alloy (Al-Si-Fe) and that reinforced with silicon carbide particles.

4) The hardness values and activation energy of diffusion obtained from aged Al-Si-Fe reinforced with silicon carbide increased with increase in the weight fraction of silicon carbide and this accelerated the kinetic to ageing.
5) The addition of SiC particles affects not only the precipitation kinetics but also the relative amounts of the various phases present in the microstructure, and that during quenching from the solution heat treatment temperature, the SiC particles cool more slowly than the matrix (since the particles have a lower thermal conductivity). This causes the matrix around the particles to be warmer than the bulk matrix. The high dislocation density and the high solubility centers (the warm particles-matrix interfaces) in the composite are favorable conditions for precipitation formation. This mechanism is a possible explanation for the higher volume fraction of precipitates obtained in the composite of the age hardening condition.
6) The kinetic parameters determined for the formation and dissolution of SiC particles are, within the limits of experimental errors, in good agreement with those obtained by the Kissinger expression.
7) The results obtained from the statistical analysis are in agreement with the experimental findings for the ageing time and temperatures. It was found that hardness increases with increasing weight fraction of silicon carbide in the alloy and decreases with increasing ageing time.

8) It is possible to produce aluminium alloy with lower silicon content by using double stir casting method and surface oxidization of the SiC particles help to improve the wettability of the SiC particles, also enhance good particle distribution and good interfacial bonding.
9) This study therefore, has established that these grade of composites response to precipitation hardening heat treatment.
10) The composites has the better properties at the ranges of 15-20% silicon carbide additions, and for optimum service condition, silicon carbide addition should be not exceeding 20% in order to have better properties.
11) Based on the resulted obtained in this study, it is recommended that this grades of composites can be used in the production of brake disc and plates.

5.2 RECOMMENDATION

The current study has yielded some important information about the microstructure and ageing behavior of Al-Si-Fe and its SiC particle-reinforced composites. In the course of the investigation, some recommendations and new areas of research have been identified.

1) It is recommended that the matrix-particle interface be investigated using high-resolution scanning electron microscopy (HRSEM) or high-resolution transmission electron microscopy (HRTEM) to reveal the presence of a reaction zone and confirm the existence of intermetallics such as $FeSiAl_3$
2) X-ray diffraction should be investigated to determine the ageing behavior of Al-Si-Fe/SiC composites and to measure the amount of Al_4C_3 formed.
3) Other mechanical properties such as fatigue and creep test should be carried out on this material.
4) Differential scanning calorimetry (DSC) experiment should be studied on this material and where possible, electrical resistivity measurements during ageing coupled with TEM examination should also be examined.

REFERENCES

Annual Books of ASTM Standards, (1990): Section 1. Iron and steel Products, volume 01 Pp 13 – 63

Asthana R (1998): Solidification processing of reinforced metals (Trans. Tech. Publ.) Pp 67-80.

Bayourni .M. Ribes .A, H. and Suéry .M (1988):"Aging Characteristics of SiC-Particle Reinforced AI-Si Alloys", Proc. 9th. Ris@ Inter. *Symp.* on Metallurgy and Materials Science, Ris@ National Laboratory, Roskilde, Denmark, Pp 291- 296.

Christman .T, Needleman. A. Nutt .S. and Suresh .S (1989): "On Microstructural Evolution and Mechanical Modeling of Deformation of a Whisker-reinforced Metal-Matrix Composite", Mater. Sci. Engr, Vol. A107, Pp 49-61.

Clyne T. W (ed.) (2000): Comprehensive composite material. *Metal matrix* Composites (ser. eds): *Vol. 3,* Pp 26-38.

Cottu.J.P, Coudere.J.J, Viguier .B and Bernard .L (1992): J.Mater Sci 27, Pp 3068-3074.

Dieter.G.E (1988): Mechanical Metallurgy, McGraw-Hill Company, Pp 184-223

Donne.S, Krishnadev.M.R and Bouchard.R (1990): Metal and ceramic matrix mechanical behavior. The minerals metals and materials society Pp243-251.

Ghosh. K.S, Das.K and Chatterjee. U.K (2004) Studies of the microstructural Changes upon retrogression and reaging (RRA) treatment to 8090 Al-Li-Cu-Mg-Zr Alloy, journals of materials science and technology vol 20 Pp 825-834

Ikechukwuka N. A. Oguocha (1997): Characterization of aluminium Alloy 2618 and Its Composites containing alumina particles, unpublished PhD thesis Department

Mechanical engineering, University of Saskatchewan, Saskatoon: Pp 1-2000.

Irwin.M and Freund.J.E (1987): Probability and statistics for engineers, Prentice Hall of India private limited Pp1-157

Jayalakshmi .S, Seshan.S Kailas.S.V, and Srivatsan.S (2004): Influence Processing and Reinforcement on microstructure and impact behaviour of magnesium alloy AM100 S¯adhan¯a Vol. 29, Part 5, October 2004, Pp 509–523. © Printed in India.

Jokinen, A. & Rauta, V (1992): Manufacturing and Properties of aluminium Alloy Matrix Composites, Final Report. Espoo: Technical Research Centre of Finland, Metallurgy Laboratory: P 26.

King. F (1987): *Aluminium and* Its Alloys, Ellis Horwood Ltd., NY P 56.

Kissinger. H. E (1957): "Reaction Kinetics in Differentid Thermal Analysis", *Anal. Chem.,* Vol. 29 No. 1, Pp 1702- 1706.

LePetitcorps.Y, J. Quenisset .M, Le Borgne GandBarthole.M (1991):"Segregation of Magnesium in Squeeze-Cast Aluminum Matrix Composites Reinforced with Alumina Fibers", *Mater. Sci Engr., A* 235, Pp 37-40.

Lloyd D J (1999): Particle reinforced aluminium and magnesium matrix Composites. *Int. Mate:* 39: Pp 1–23.

Lloyd .D. J, Lagace .H. P. and McLeod . A. D (1990): "Interfacial Phenornena in Metal Matrix Composites", Controlled Interphases in Composite Materials, Elsevier Science Pub. CO., N. Y., Pp 359-376.

Markandeya.R, Nagarjuna .S and Sarma.D.S (2004): Precipitation hardening of Cu- Ti-Zr alloys, journals of materials science and technology vol 20 Pp 849-858

Maruyama B (1998): Progress and promise in aluminium metal matrix composites, *the AMPTIAC* Newsletter: P 23.

Mbaya.E. I (2005), The development of dispersion strengthened Tin-silica composite used as a material for plain bearings, M.S.C Thesis department of mechanical engineering , ATBU Bauchi

McDanels .D. L (1985): "Analysis of Stress-Strain, Fracture, and Ductility of Aluminum Matrix Composites Containing Discontinuous Silicon Carbide Reinforcement", *Metall. Trans. A,* Vol. 16A7 Pp 105-115.

Metals Handbook (1979): Properties and selection of Non ferrous alloys and pure metals. American Society of metals (ASM) Pp 45-67.

Metals handbook (1985): mechanical testing, 9th edition, volume 8, American society for metals, the united states of America Pp 250-257

Mittemeijer .E. J., Cheng .L. van der Schaaf. P. J., Brakrnan. C. M. and Kcxevaar, B. M (1998): "Analysis of Non-isothermal Transformation Kinetics; Tempering of Iron-Carbon and Iron-Nitrogen Martensites" Metall. Trans. A, 19A Pp 925-932.

Miesel .L. V. and Cote .P. J(1983): "Non-Isothemal Transformation Kinetics: Application to Metastable Phases", Acta. Metall., 3 l(7) Pp 1053- 1059.

Nardone .V. *C.* and Prewo. K. M(1986) : "On the Strength of Discontinuous Silicon Carbide-Reinforced Aluminium Composites", *Scripta Metall.,* Vol. *20,* Pp 43-48.

Nieh .T. G. and Karlak R.F(1984): "Aging Characteristics of B4C-Reinforced 6061-Aluminum", Scripta Metail., Vol. 18, Pp 25-28.

Padkin. A. J. Boreton .M. F., and Plumbridge .W. J(1987):"Fatigue Crack Growth in Two-Phase Alloys", Mater. *Sci.* Tech., Vol. 3, Pp 2 17-223.

Piggott .M. R(1980): *Load Bearing Fibre Composites.* Oxford, Pergamon Press P 89.

Rajan .TV and Sharma C.P (1988) Heat treatment principles and techniques, Published by prentice-hall of India private limited Pp 35-159.

Ramachandra.M and Radhakrisha. K (2006): Sliding Wear, Slurry Erosive Wear and Corrosive Wear of aluminium/SiC Composites J. Materials Science, Poland, vol 24, Pp 333-349

Ribes .H, Suéry. M, L'espérance .G. and Legoux. J. G (1990):"Microscopic Examination of the Interface Region in 6061-AVSiC Composites Reinforced With As-Received and Oxidized 6061 Al/SiC Particles", *Metall. Trans. A,* Vol. 21, Pp 2489-2496.

Rohatgi P.K., F.M. Yarandi and Y. Liu, (1988): Proc. of Inter. Symposium on Advances in Cast Reinforced Metal Composites (S.G. Fishman and A.K. Dhingra, eds.), Materials Park, OH: ASM International Publication: P 249

Sagail A., Leisk G (1992): Heat treatment optimization of Alumina/Aluminium Metal Matrix Composites using the Taguchi approach Scripta Metallurgica et Material Pp 871-876

Shi.N.and Arsenault. R. J (1994): "Plastic Flow in SiC/Al Composites–Strengthening and Ductility", Ann. *Rev.* Mater. Sci., Vol. 24, Pp 321-357.

Skibo.M, Morris. P. L and Lloyd .D.J (1988): Cast reinforced composites S.G Fishman and A.K Dhirngra (eds) ASM International Pp257-261.

Starink . M. J. and van Mourik. P(1992): "Cooling and Heating Rate Dependence In an *Al*-Cu Alloy", *Mater. Sci. Engr.,* A156 Pp 183-194.

Song S. G., Shi. N, Gray III .G. T and Roberts .J. A(1996):"Reinforcement Shape Effects on the Fracture Behavior and Ductility of Particulate-Reinforced 606 1 -*Al* Matrix

Composites", Metall. and Mater. Trans. *A,* Vol. 27A, Pp 45-55

Song .Y. and Baker .T. N(1994): "Accelerated Aging Processes in Ceramic Reinforced AA 6061 Composites", Mater. *Sci.* Tech., Vol. 10, Pp 3739-3746.

Srivatsan.T.S and Mattingly.J (1993): J. Mater Sci, 289 Pp 611-620

Surappa M K, Rohatgi P K (1981): Preparation and properties of aluminium alloy Ceramic *particle composites. J. Mater. Sci. 16: Pp 983–993.*

Vergaard. V. T(1990):"Analysis of Tensile Properties for a Whisker-Reinforced Metal-Matrix Composite", Acta Metall. et Mater., Vol. 38, Pp185-194.

Vogelsang. M. Arsenault .R. J. and Fisher .R. M(1986):"An In-Situ HVEM Study of Dislocation Generation at Al/SiC Interfaces in Metal Matrix Composites", Metall. Trans. A, Vol. 17A, Pp 379-389.

Watt .D. F, Xu. X. Q. and Lloyd .D. J(1996):"Effects of Particle Morphology and Spacing on the Strain Fields in a Plastically Deforming Matrix", Acta Mater., Vol. 44, Pp 789

Whitehouse A. F, Shahani, R. A. and Clyne .T. W(1991): Metal Matrix Composites: Processing, Microstructure *and* Properties, *12 Ris*θ Int. *Symp.,* Roskilde, N.Hansen et al., eds, Risθ National Laboratory, Denmark, Pp 74 1-748.

Wendlandt . M. B. X, Barnard . J. A., Ramanujan . R. V. and Aaronson. H. I(1986): "A Critique of Activation Energies for Nucleation Growth and Overall Transformation Kinetics", *Scripta* Metall., 20 Pp 323-328.

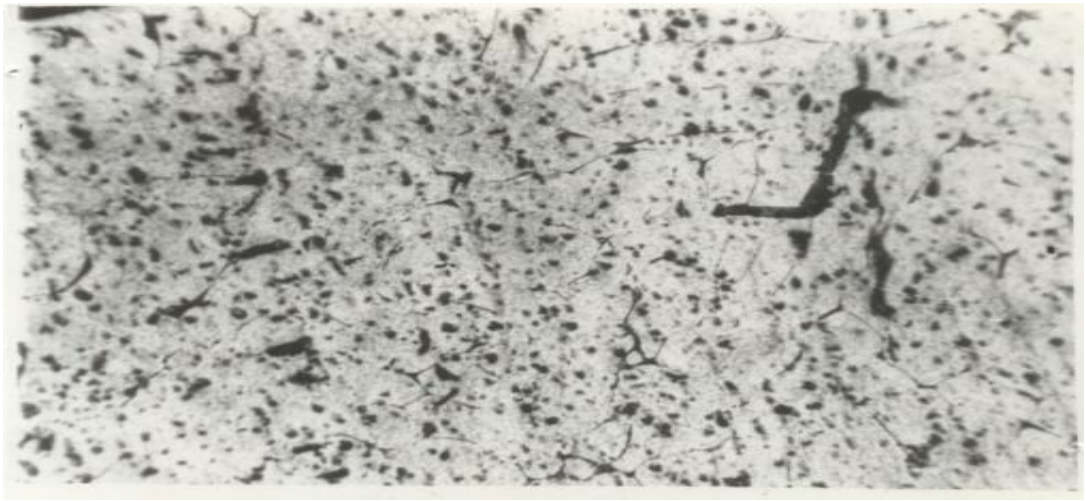
Xu . X. *Q.* and Watt . D. F(1996): " Numerical Analysis of the Effects of Reinforcement Content on Strength and Ductility in AlSiCp MMCs", *Acta* Mater., Vol. 44(1 l), Pp 4501-45 11

Zhou, W. and Xu .Z.M(1997): Casting of SiC Reinforced Metal Matrix, *Journal of Material*s Processing Technology 63: Pp *358-363*

APPENDIX A (MICROGRAPHS)



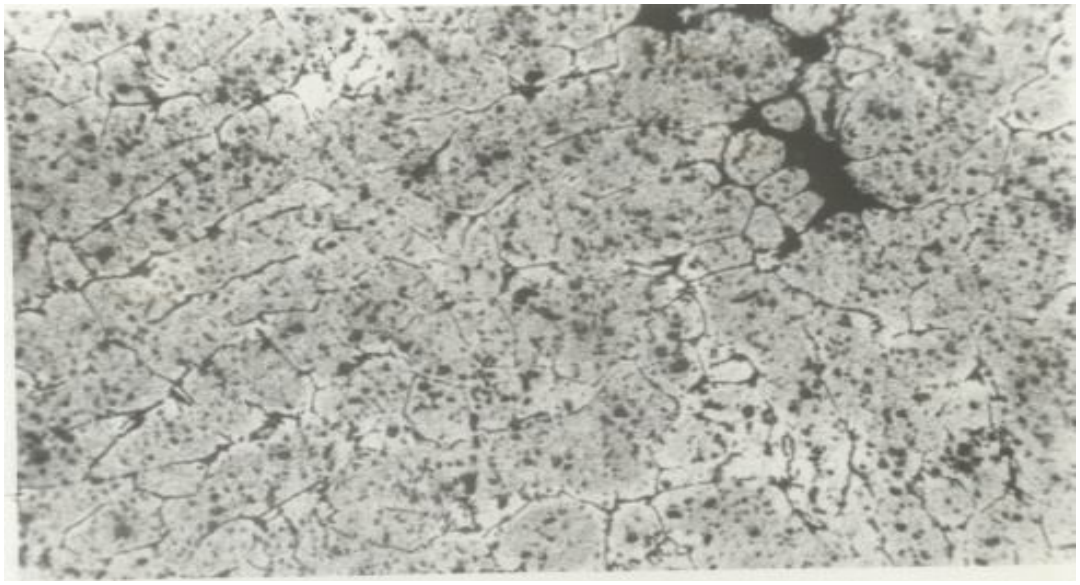
Micrograph A1, Microstructure of the Al-Si-Fe alloy, showing silicon eutectic (black) containing $FeAl_3Si$ phases and α-Al (white) (x200). The structure reveals the eutectic silicon containing $FeSiAl_3$ phase in aluminium matrix.



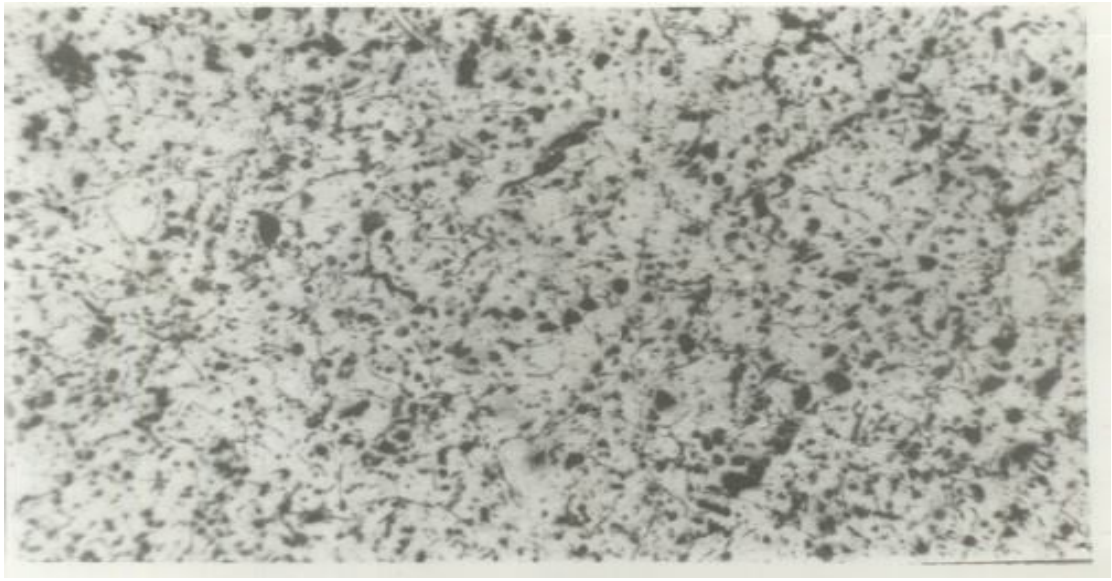
Micrograph A2: Microstructure of Al-Si-Fe alloy reinforced alloy with 5 wt% of SiC. The structure reveals the dissolution of the eutectic silicon phase and slight agglomeration of SiC in microscale (black) in α-Al matrix (white) (x200)



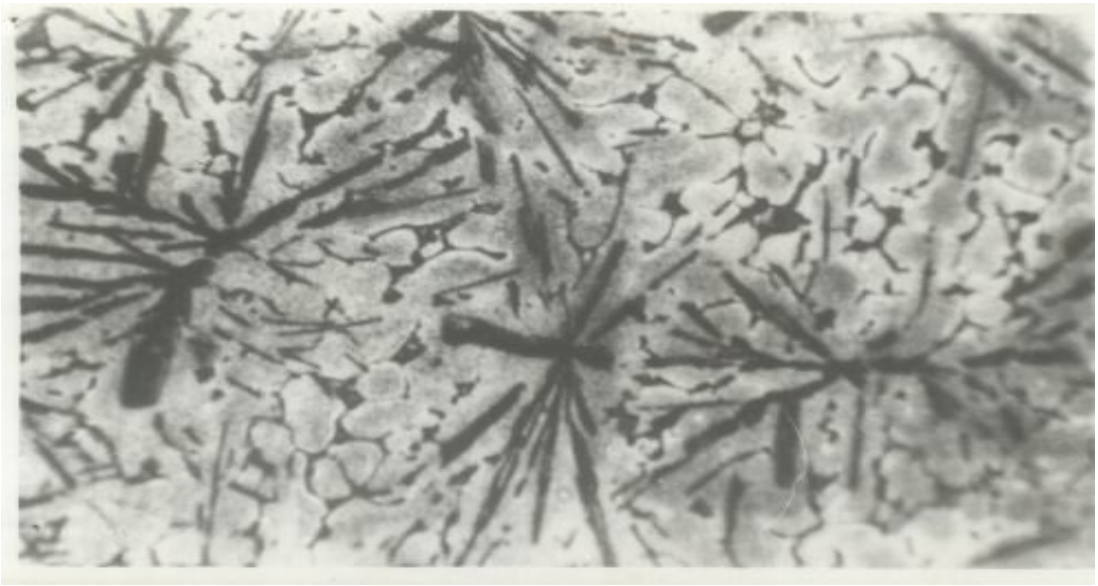
Micrograph A3: Microstructure of Al-Si-Fe alloy reinforced alloy with 10 wt% of SiC the structure reveals the dissolution of the eutectic silicon phase and uniform distribution of SiC (black) in α-Al matrix (white) (x200)



Micrograph A4: Microstructure of Al-Si-Fe alloy reinforced with 15 wt% of SiC. The structure reveals the Dissolution of the eutectic Silicon phase and uniform distribution of SiC (black) (x 200)

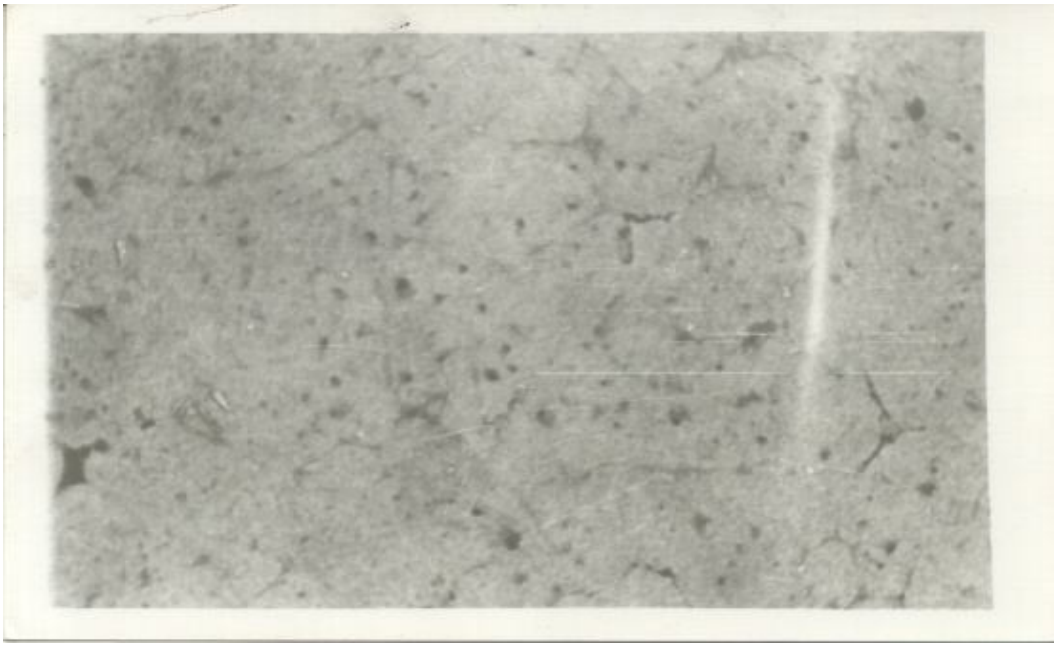


Micrograph A5: Microstructure of Al-Si-Fe alloy reinforced with 20 wt% of SiC. The structure reveals the dissolution of the eutectic silicon phase and uniform distribution of SiC (black) in α-Al matrix (white) (x200)



Micrograph A6: Microstructure of Al-Si-Fe alloy reinforced with 25 wt% of SiC.

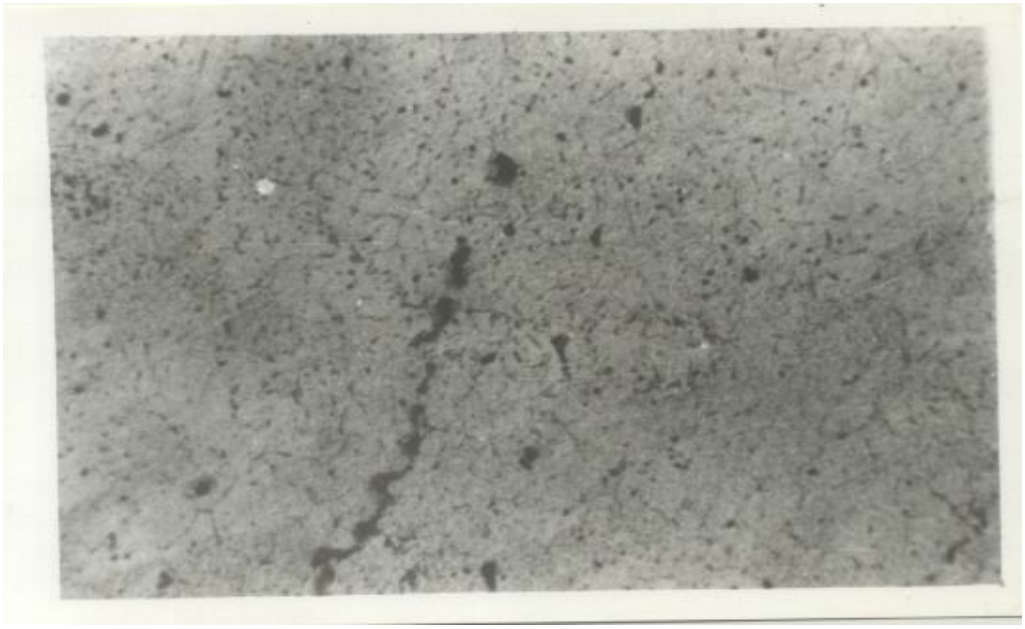
The structure reveals dissolution of the eutectic silicon phase, segregation and agglomeration of SiC particles(black) in α-Al (white) (x200)



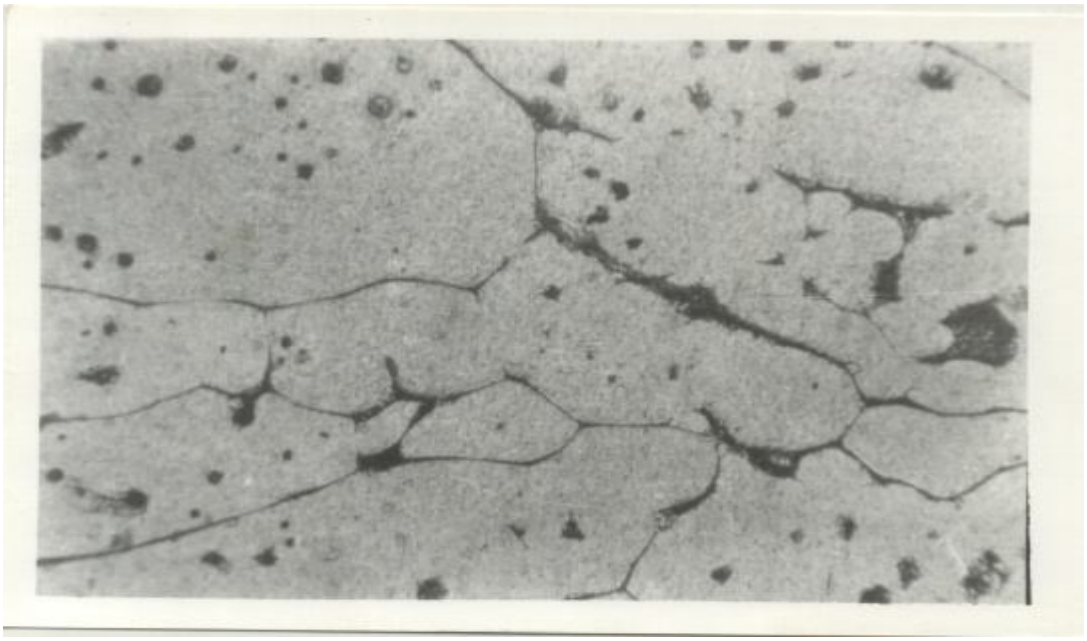
Micrograph A7: Microstructure of the Al-Si-Fe alloy after peak aged at $100^{O}C$ (x200).The structure reveals dissolution and precipitation of the silicon eutectic(black) and the $FeAl_3Si$ Phases in α-Al matrix (white)



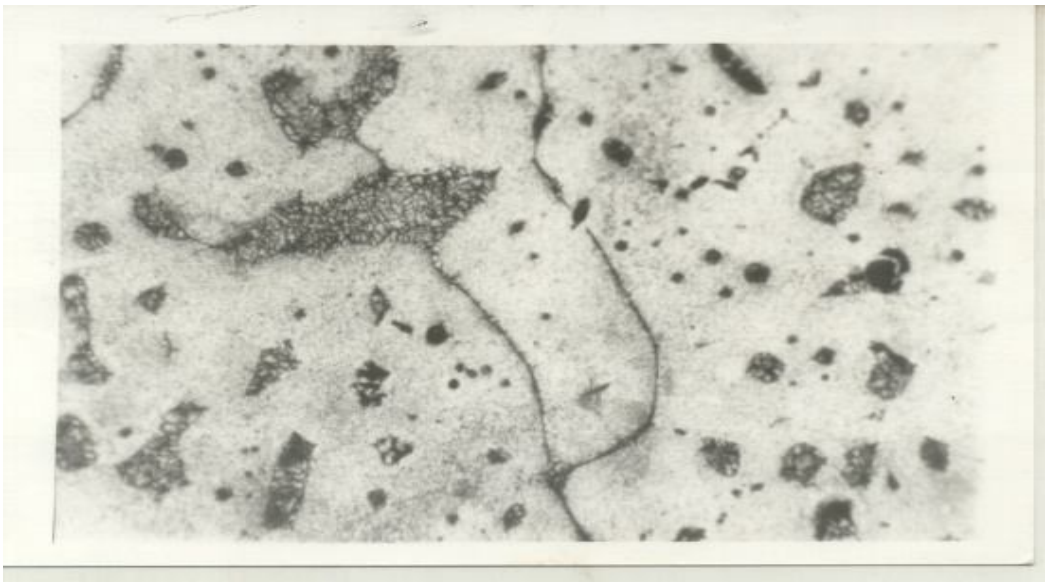
Micrograph A8: Microstructure of the Al-Si-Fe alloy after peak aged at $200^{O}C$ (x200) The structure reveals uniform dissolution and precipitation of the silicon eutectic (black) and the $FeAl_3Si$ Phases in α-Al matrix (white)



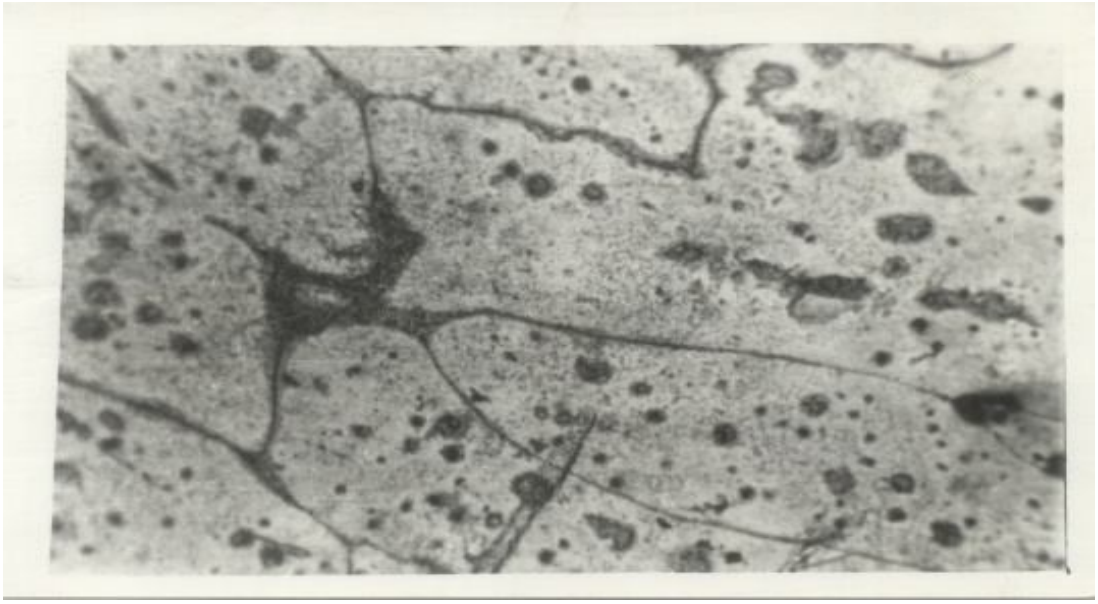
Micrograph A.9: Microstructure of the unreinforced alloy after peak aged at $300^{O}C$ (x200). The structure reveals dissolution and precipitation of the silicon eutectic (black) and the $FeAl_3Si$ Phases with some segregation of silicon eutectic phases in α-Al matrix (white)



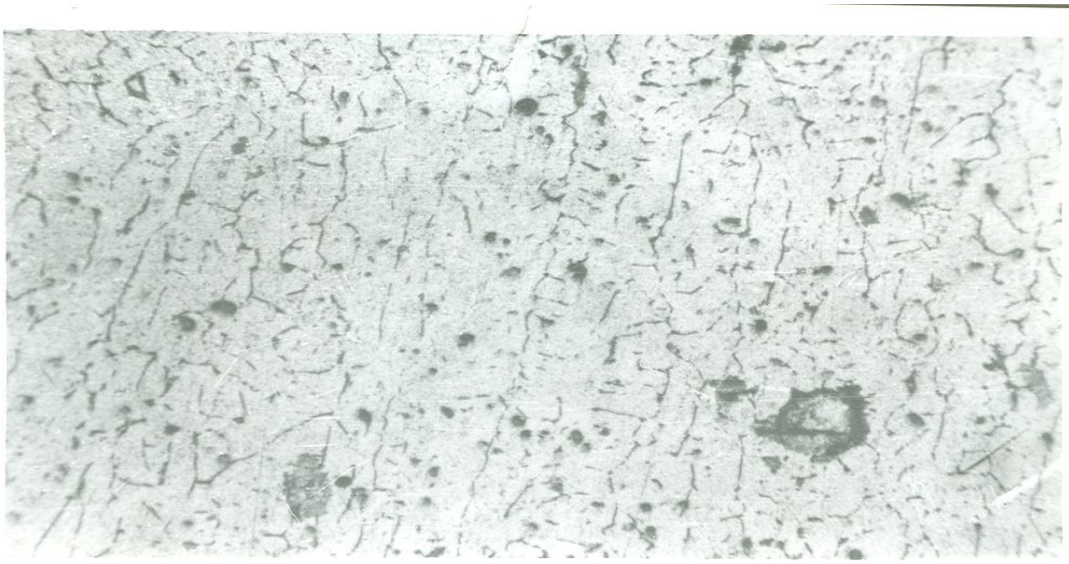
Micrograph A10: Microstructure of the reinforced alloy(5 wt% of SiC) after peak aged at $100^{O}C$ (x200). The structure reveals the dissolution and precipitation of the SiC particles (black) in α-Al matrix (white)



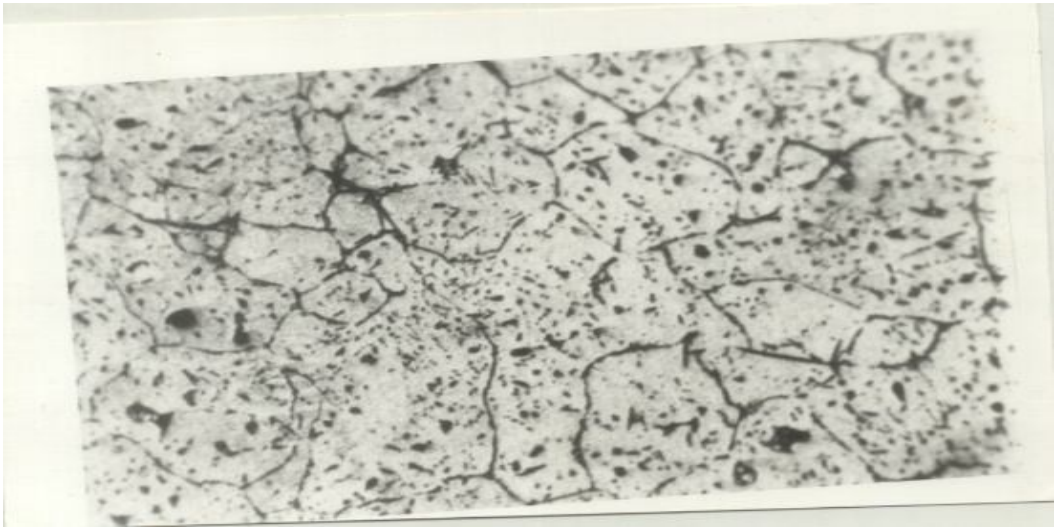
Micrograph A11: Microstructure of the reinforced alloy(5 wt% of SiC) after peak aged at 200^{O}C (x200). The structure reveals the randomly dissolution and precipitation of the SiC particles (black) in α-Al matrix (white)



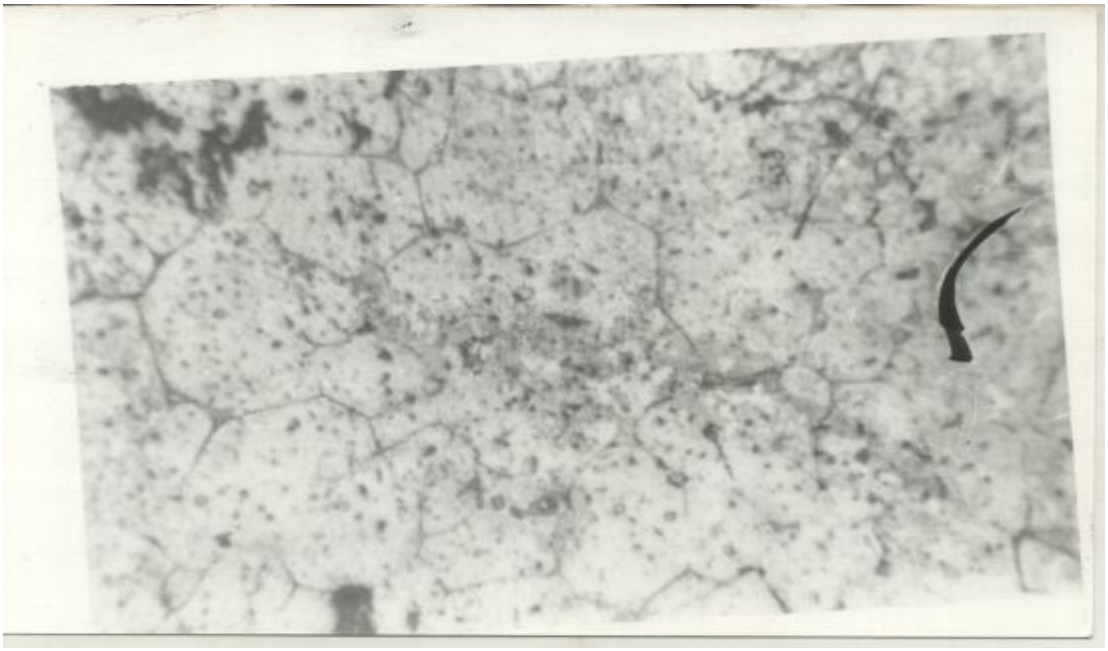
Micrograph A12: Microstructure of the reinforced alloy(5 wt% of SiC) after peak aged at 300^{O}C (x200). The structure reveals the dissolution and precipitation of the SiC particles (black) in α-Al matrix (white)



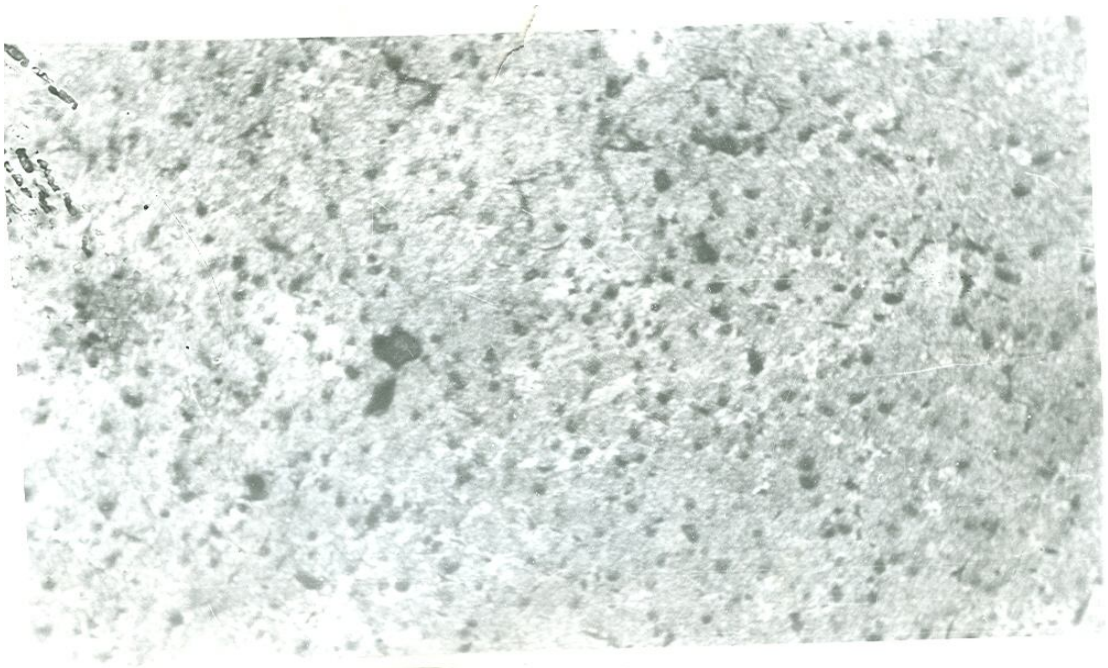
Micrograph A13: Microstructure of the reinforced alloy(10 wt% of SiC) after peak aged at 100^{O}C (x200). The structure reveals the dissolution of the eutectic silicon phase and uniform distribution of SiC (black) in α-Al matrix (white)



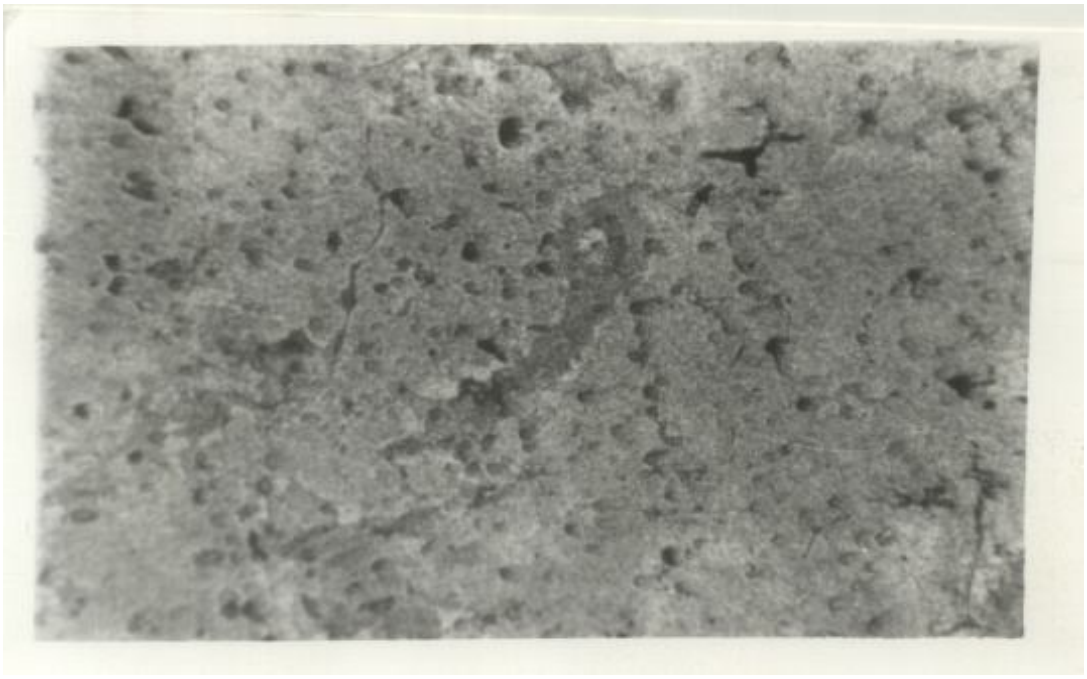
Micrograph A14: Microstructure of the reinforced alloy(10 wt% of SiC) after peak aged at 200^{O}C (x200). The structure reveals the dissolution of the eutectic silicon phase and distribution of SiC (black) in α-Al matrix (white)



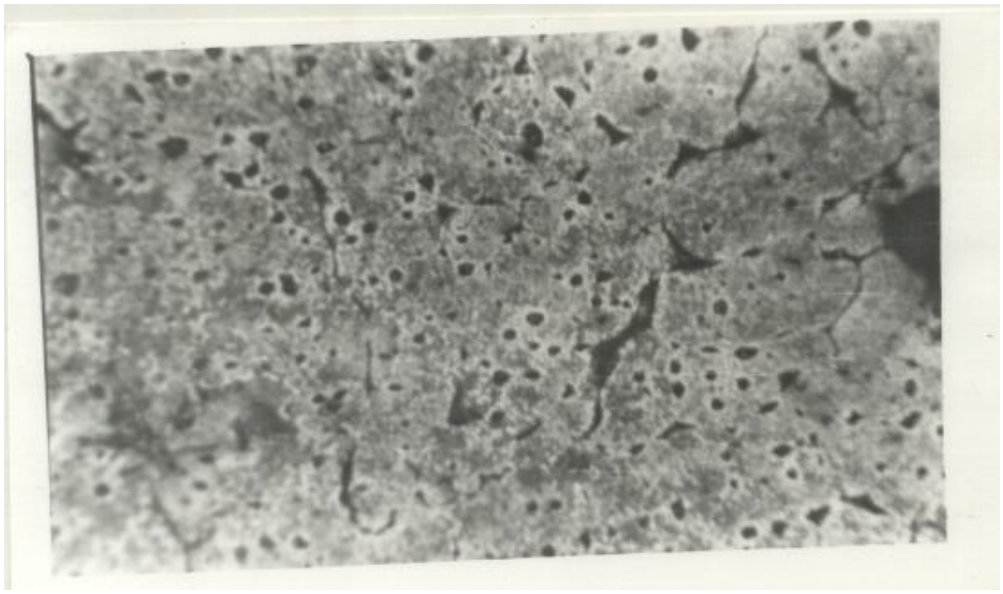
Micrograph A15: Microstructure of the reinforced alloy(10 wt% of SiC) after peak aged at $300^{O}C$ (x200).The structure reveals the dissolution of the eutectic silicon phase and uniform distribution of SiC (black) with precipitation of the SiC particles



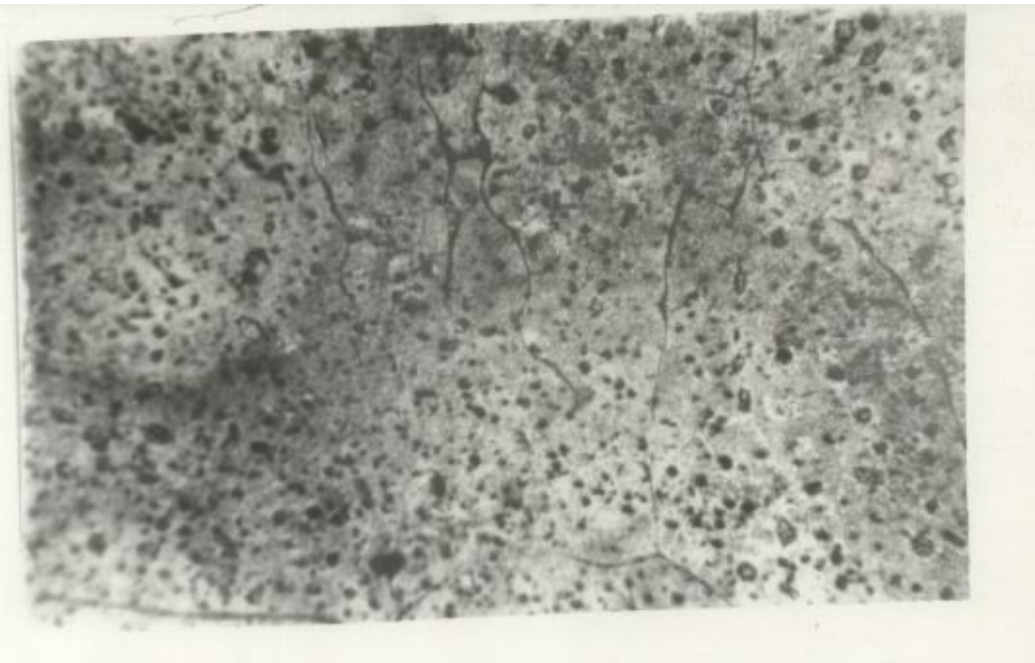
Micrograph A16: Microstructure of the reinforced alloy(15 wt% of SiC) after peak aged at $100^{O}C$ (x200). The structure reveals the dissolution and precipitation of the eutectic silicon phase and uniform distribution of SiC (black)



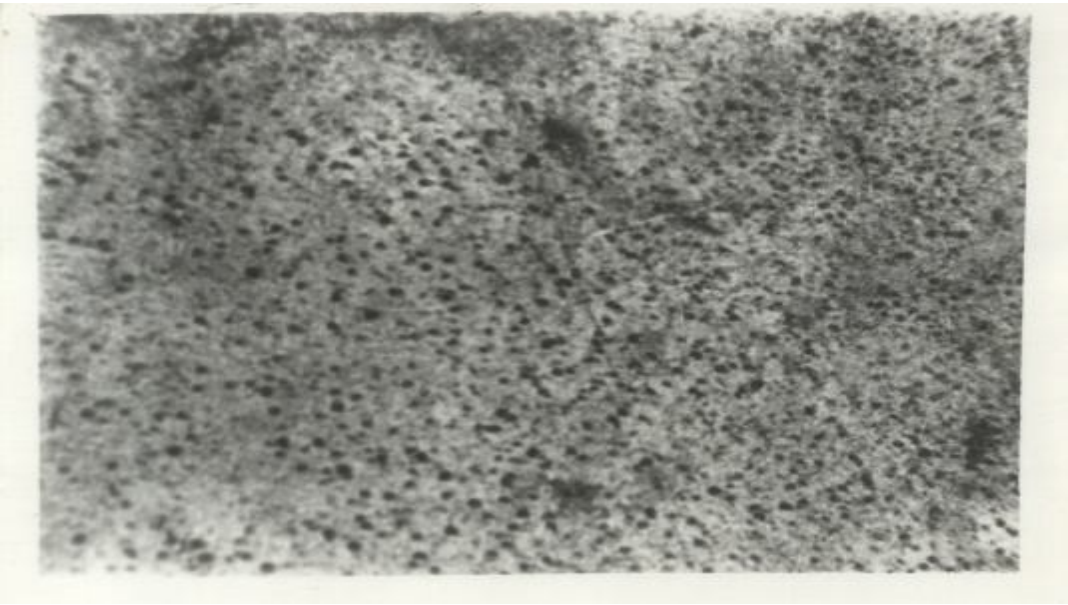
Micrograph A17: Microstructure of the reinforced alloy(15 wt% of SiC) after peak aged at 200^{O}C (x200). The structure reveals the dissolution and precipitation of the eutectic silicon phase and uniform distribution of SiC (black) with precipitation covering the α-Aluminium matrix



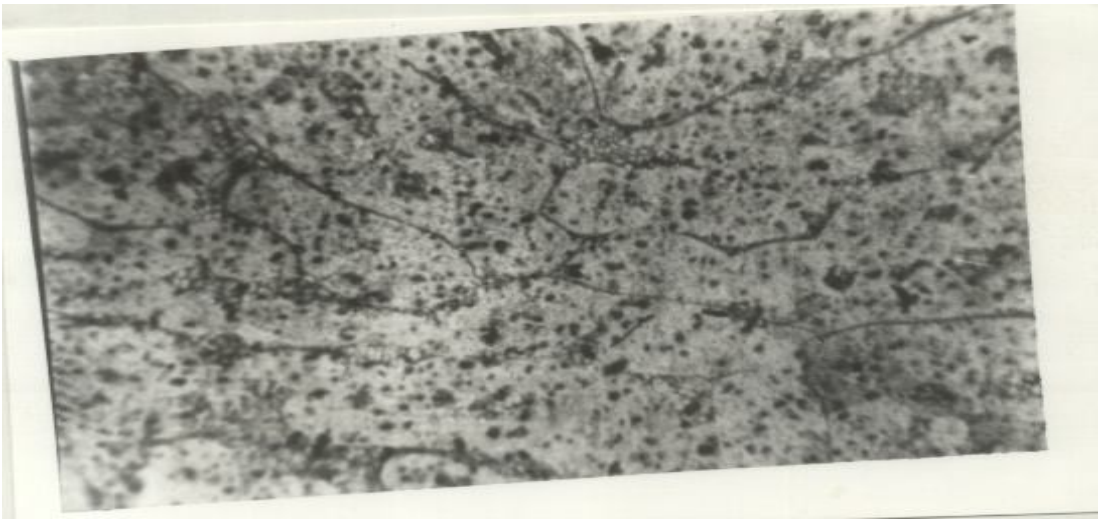
Micrograph A18: Microstructure of the reinforced alloy(15 wt% of SiC) after peak aged at 300^{O}C (x200). The structure reveals the dissolution and precipitation of the eutectic silicon phase and uniform distribution of SiC (black)



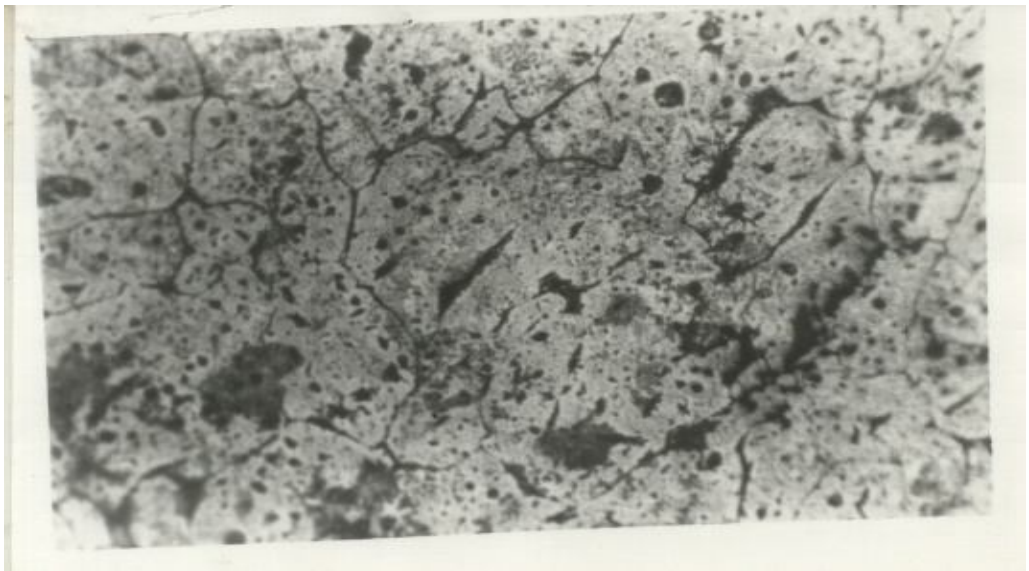
Micrograph A19: Microstructure of the reinforced alloy(20 wt% of SiC) after peak aged at $100^{O}C$ (x200). The structure reveals the dissolution of the eutectic silicon phase and uniform distribution of SiC (black) with precipitation covering



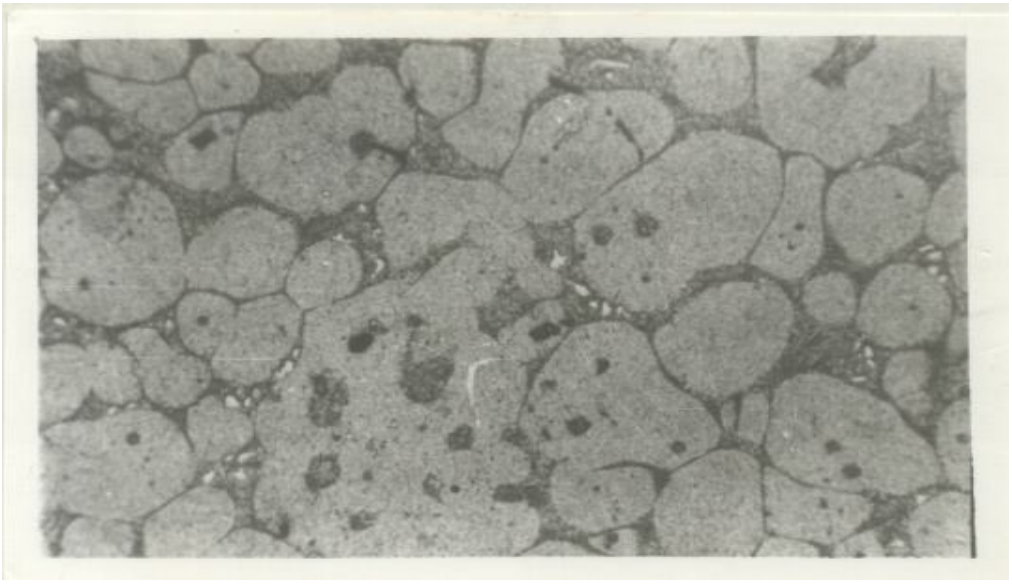
Micrograph A20: Microstructure of the reinforced alloy(20 wt% of SiC) after peak aged at $200^{O}C$ (x200). The structure reveals the dissolution of the eutectic silicon phase and well uniformly distribution of SiC (black) with precipitation covering the aluminium phase(white)



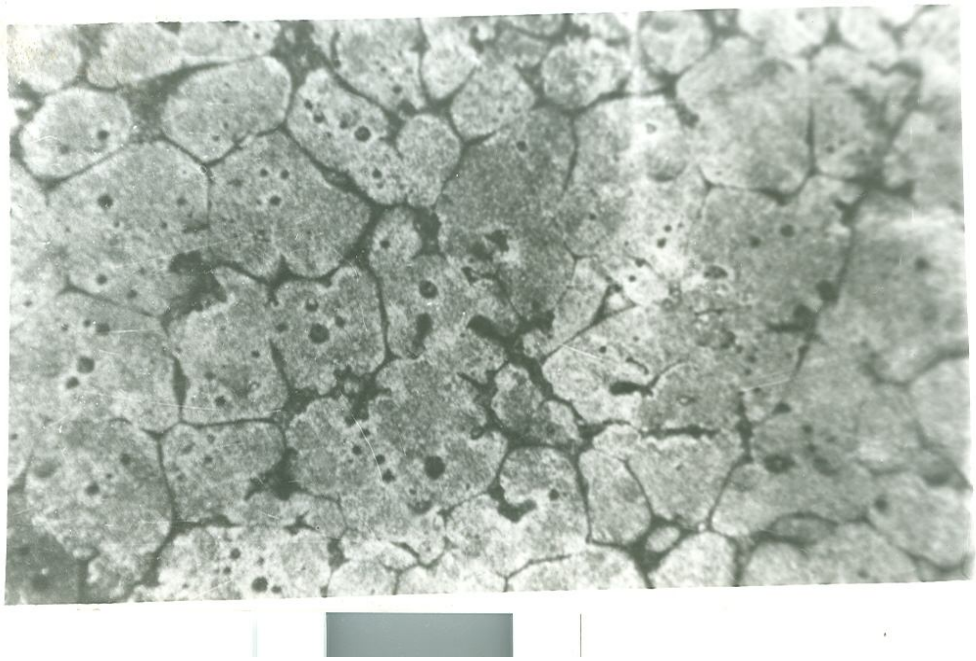
Micrograph A21: Microstructure of the reinforced alloy(20 wt% of SiC) after peak aged at $300^{O}C$ (x200).The structure reveals the dissolution of the eutectic silicon phase and uniform distribution of SiC (black) with precipitation covering



Micrograph A22, Microstructure of the reinforced alloy(25 wt% of SiC) after peak aged at $100^{O}C$ (x200). The structure reveals the dissolution of the eutectic silicon phase, precipitation of the segregation and agglomeration of the SiC particles (black)



Micrograph A23, Microstructure of the reinforced alloy(25 wt% of SiC) after peak at 200^{O}C (x200). The structure reveals the dissolution of the eutectic silicon phase, precipitation of the segregation and agglomeration of the SiC particles (black) and aluminium phase(white)



Micrograph A24, Microstructure of the reinforced alloy(25 wt% of SiC) after peak aged at 300^{O}C (x200). The structure reveals the dissolution of the eutectic silicon phase, precipitation of the segregation and agglomeration of the SiC particles (black)

APPENDIX B (FIGURES)

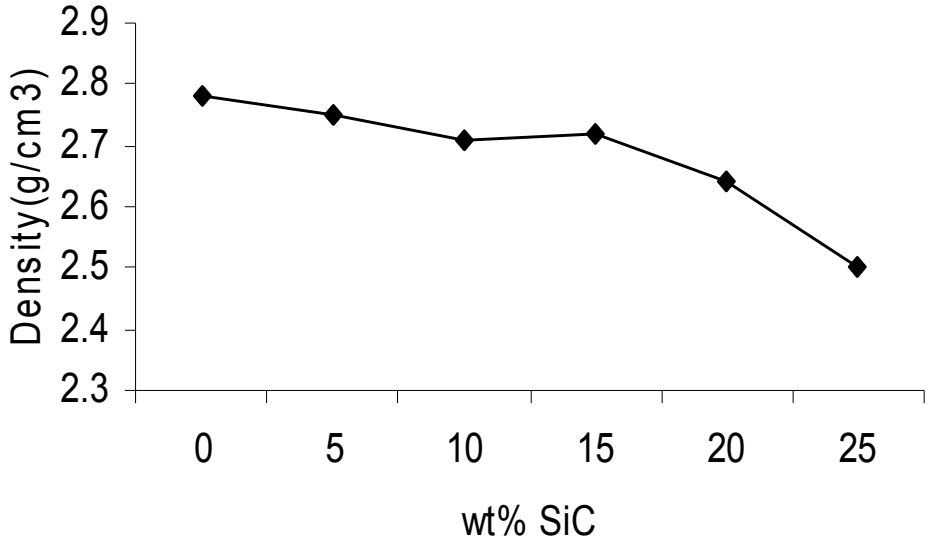


Figure B1: Variation of density with weight percentage of SiC

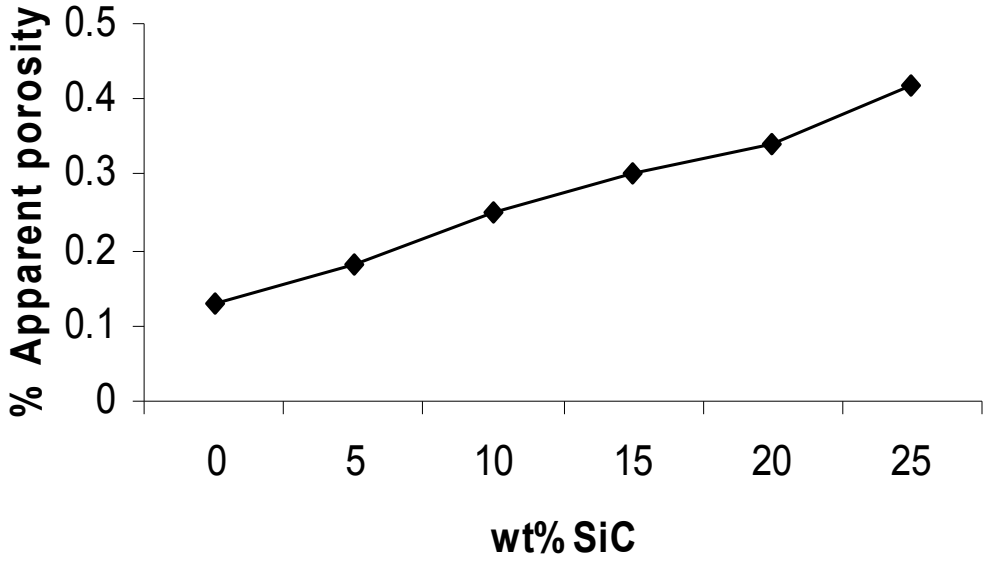


Figure B2: Variation of percentage of porosity with weight percentage of SiC

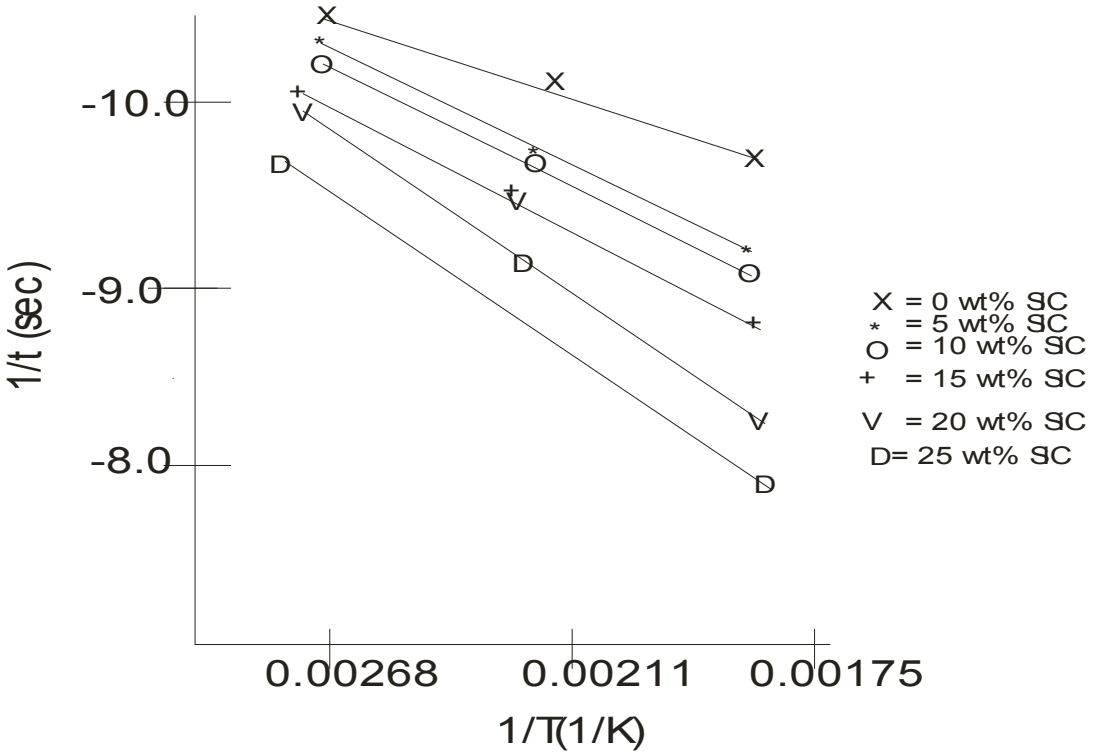


Figure B3, Plot of 1/t (sec) against 1/T (1/K) used for Arrhenius analysis

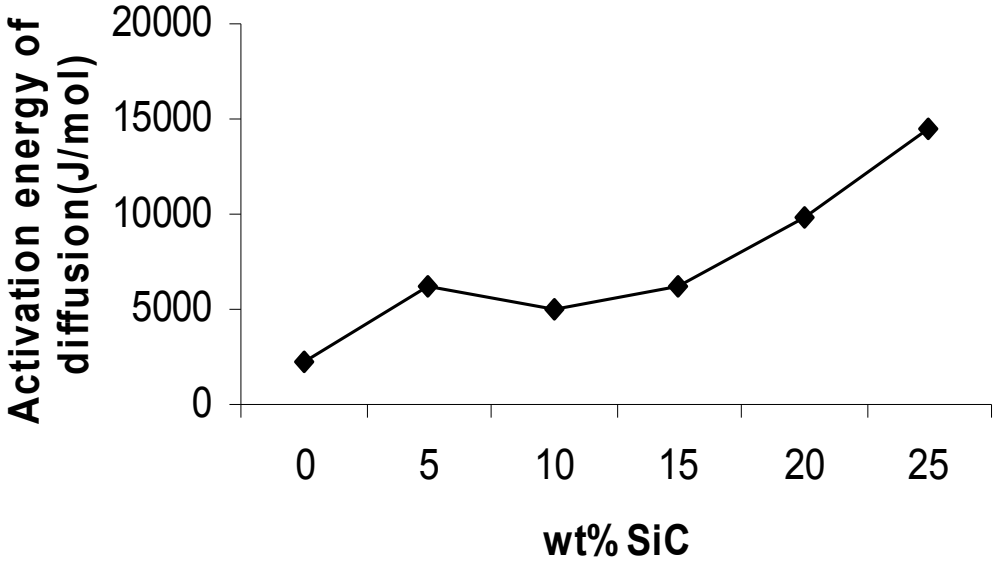


Figure B4: Variation of activation energy with weight fraction of SiC

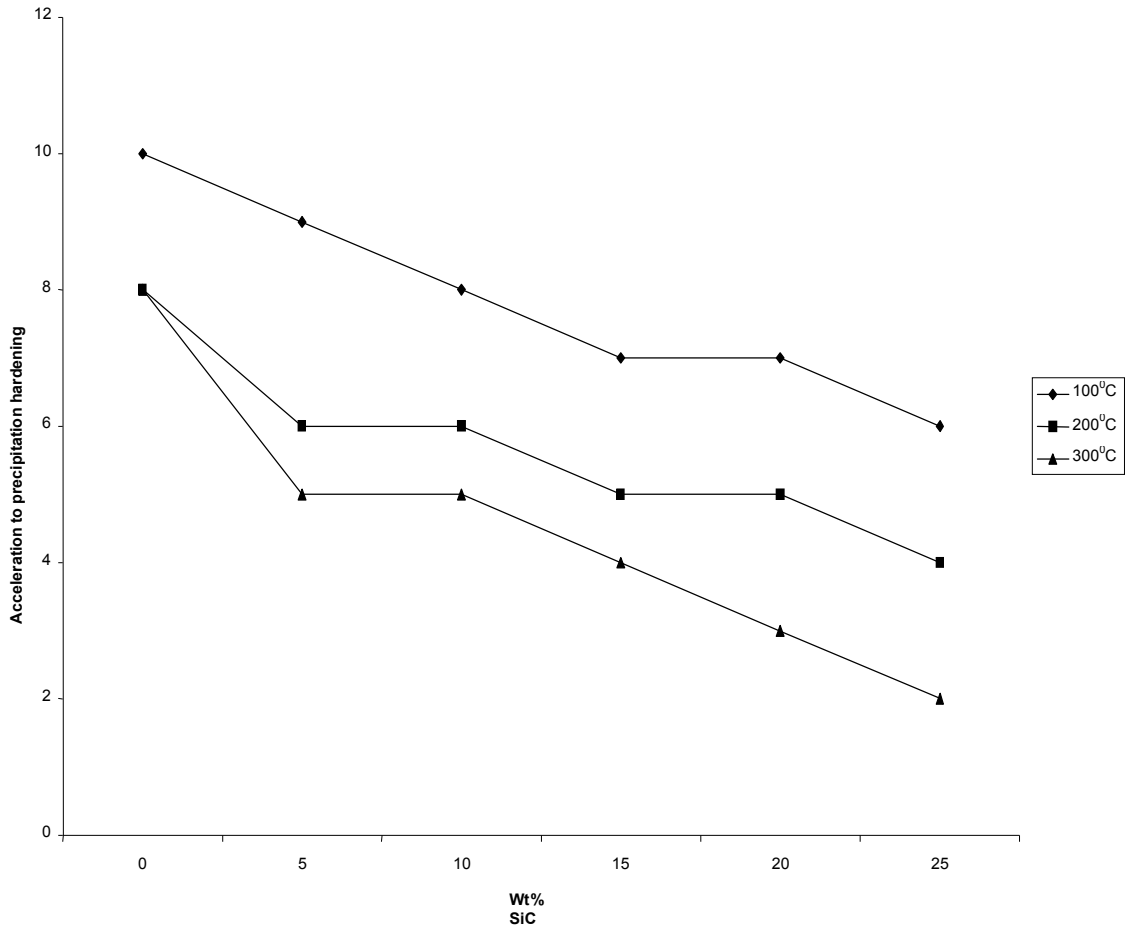


Figure B5: Variation of acceleration to precipitation hardening with weight fraction of SiC at various ageing temperatures

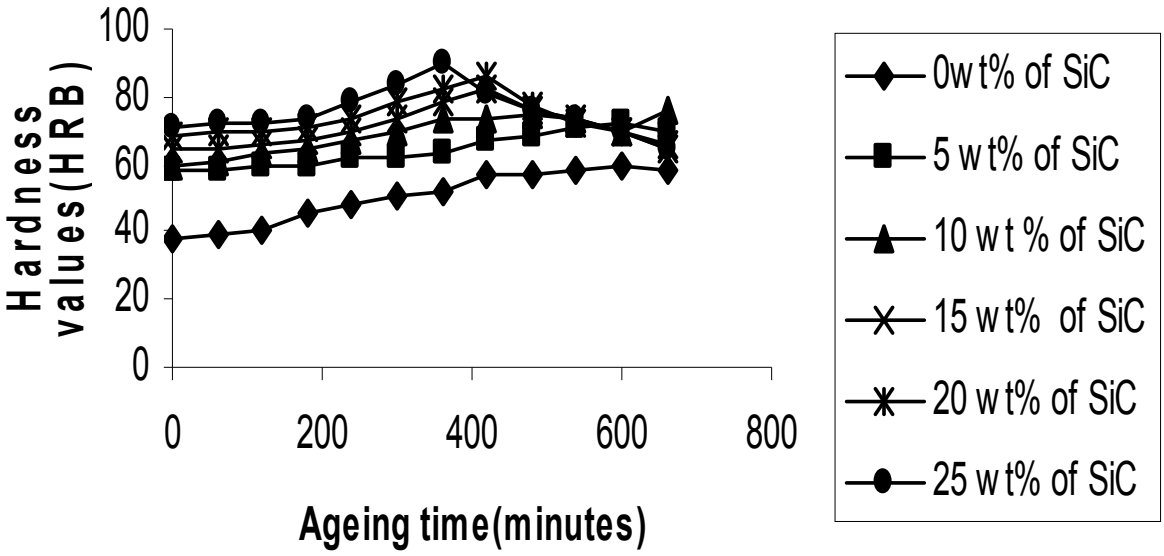


Figure B6: Variation of hardness values with ageing time of the various grades composites at ageing temperature of 100°C

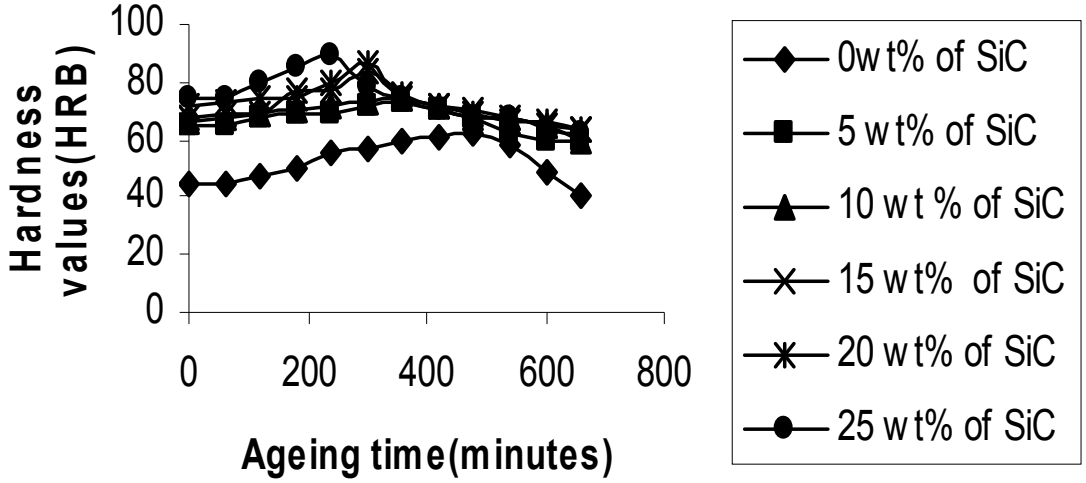


Figure B7: Variation of hardness values with ageing time of the various grades composites at ageing temperature of 200°C

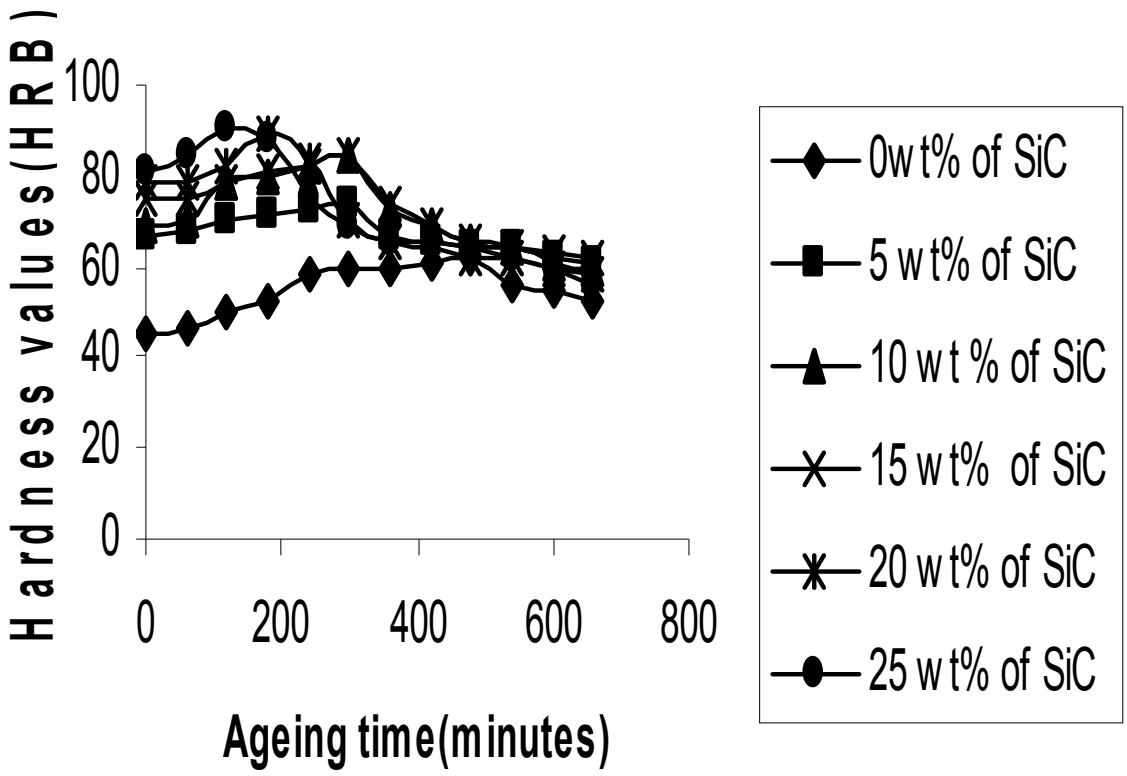


Figure B8: Variation of hardness values with ageing time of the various grades composites at ageing temperature of 300^{o}C

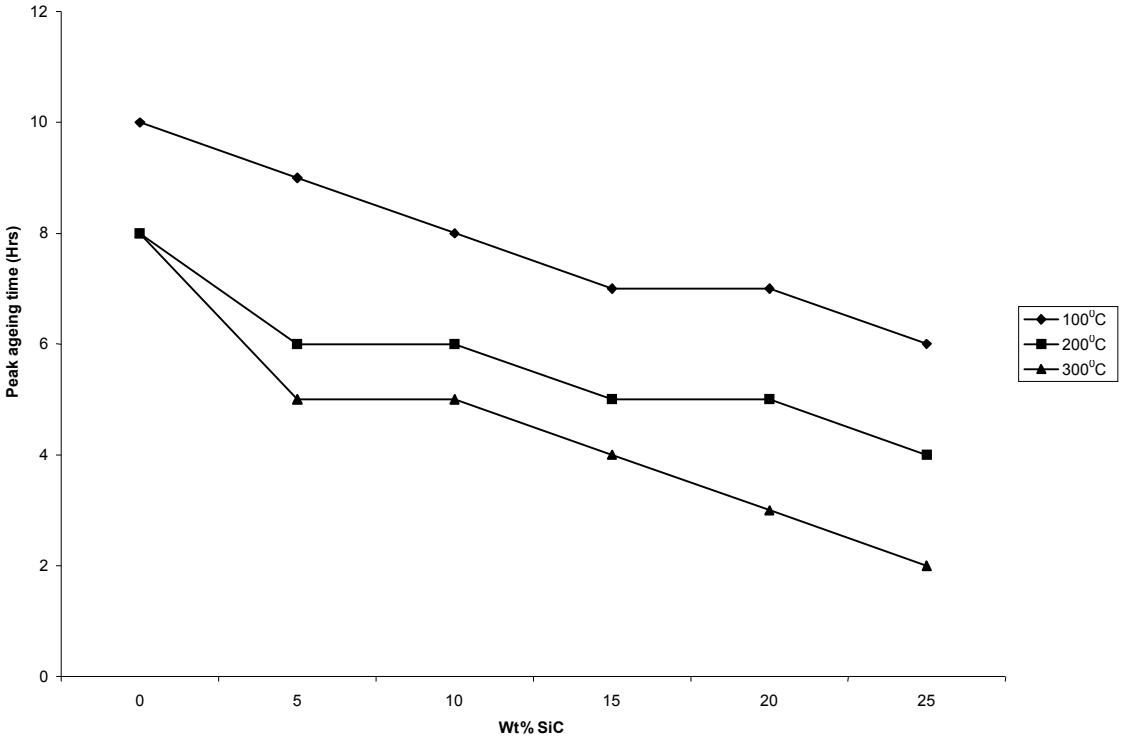


Figure B 9: Variation of peaking ageing time with weight fraction of SiC at various ageing temperatures

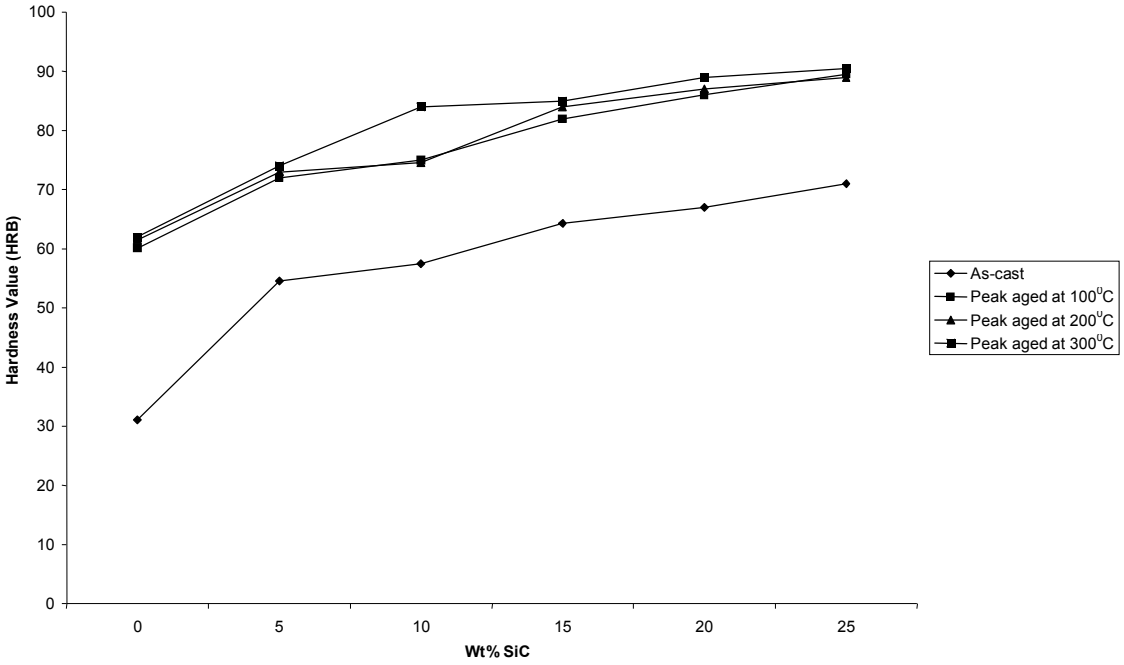


Figure B10: Variation of hardness values with weight fraction of SiC

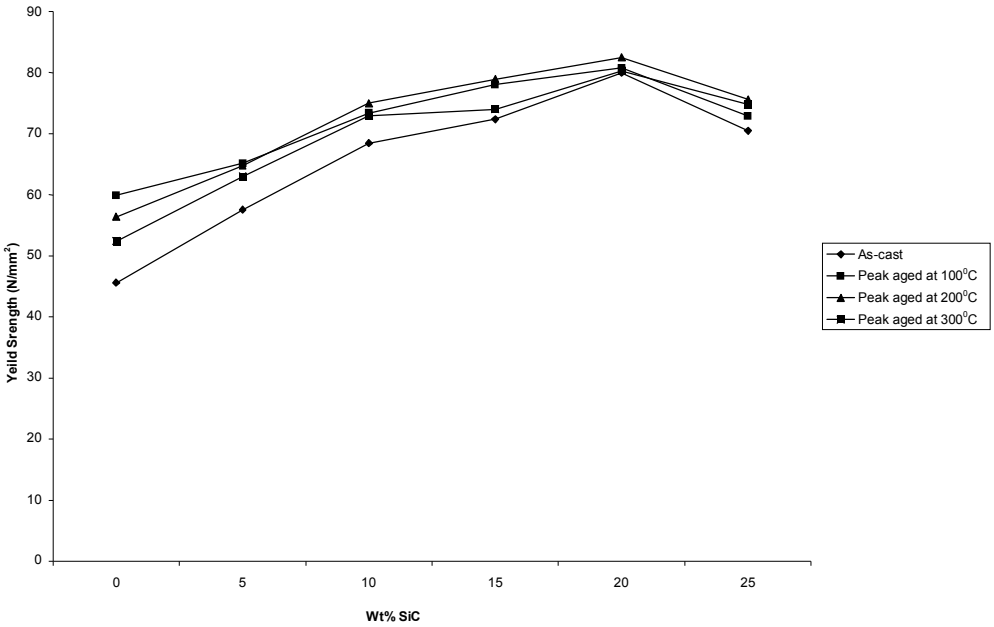


Figure B11: Variation of Yield strength with weight fraction of SiC

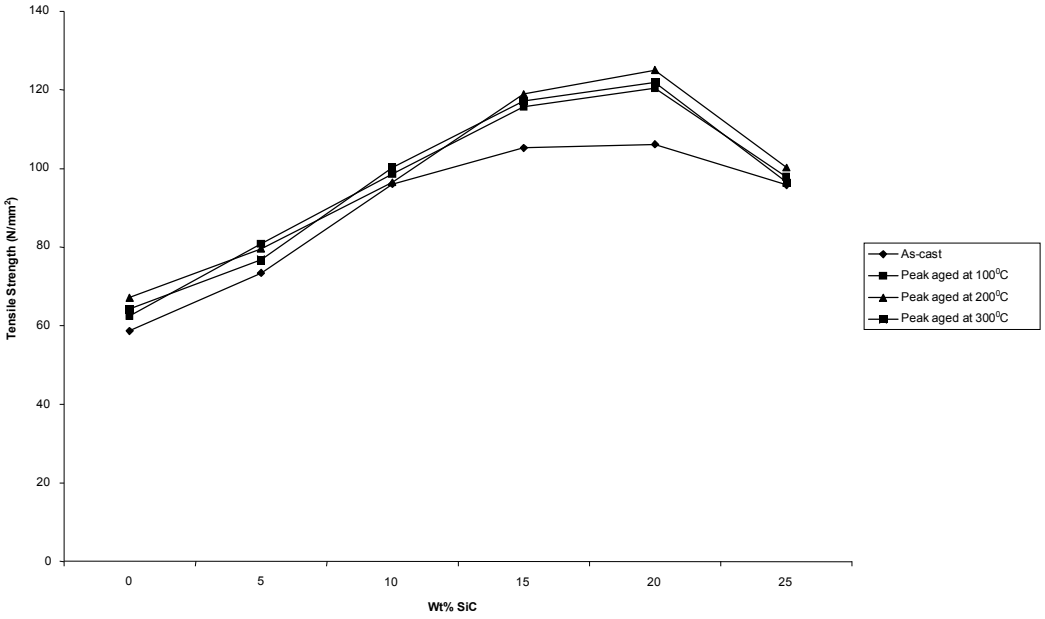


Figure B12: Variation of Tensile strength with weight fraction of SiC

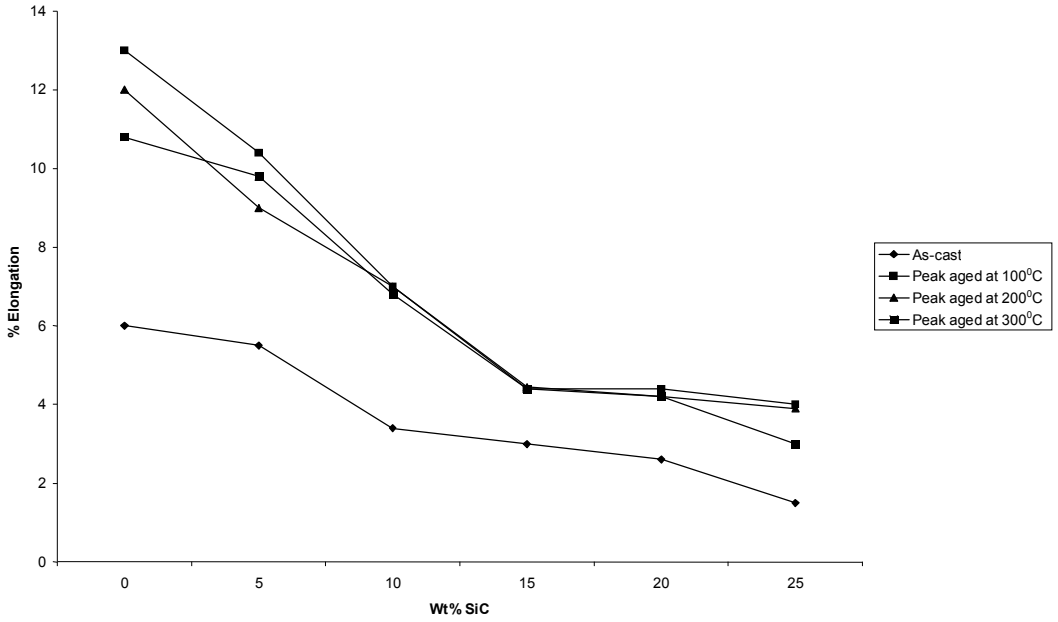


Figure B13: Variation of percentage elongation with weight fraction of SiC

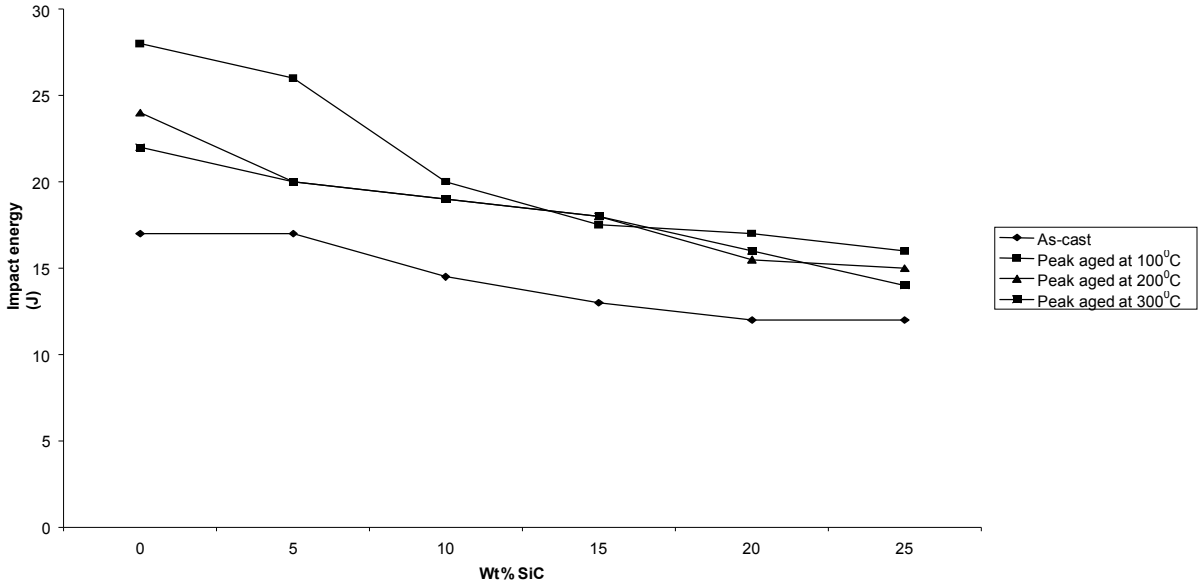


Figure B14: Variation of impact energy with weight fraction of SiC

APPENDIX C (PLATES)

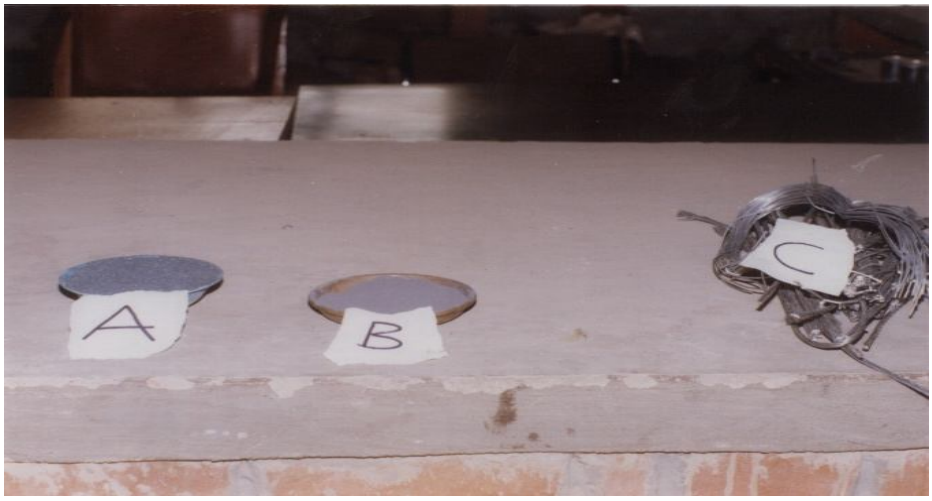


Plate C1, Materials used in the production of the composites
A=SiC, B= FeSi, C = Pure (Al)



Plate C2, After pouring of the molten mixture in the prepared sand mould



Plate C3, the produced samples after shaking from the mould

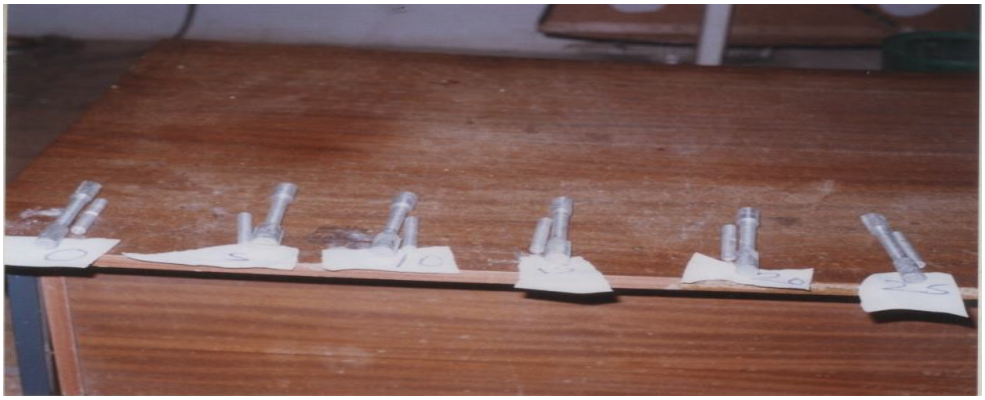


Plate C4, macrostructure of the composites after machined for mechanical test